

# **Can we use isomeric yield ratios to study the impact of nuclear level densities?**

Stephan Pomp, Ali Al-Adili, Simone Cannarozzo, Mattias Lantz, Andreas Solders

Department of physics and astronomy

Uppsala University

Sweden



UPPSALA  
UNIVERSITET

# Outline

Why measure isomeric yield ratios from fission?

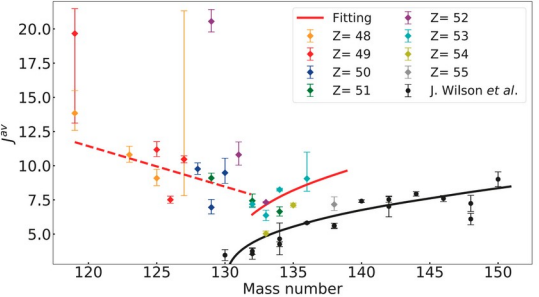
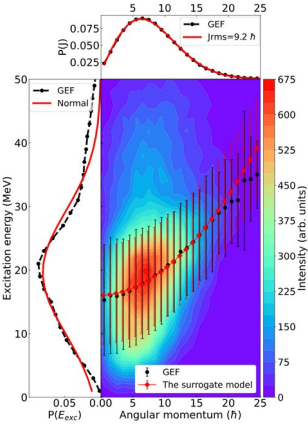
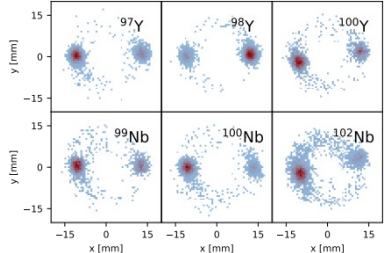
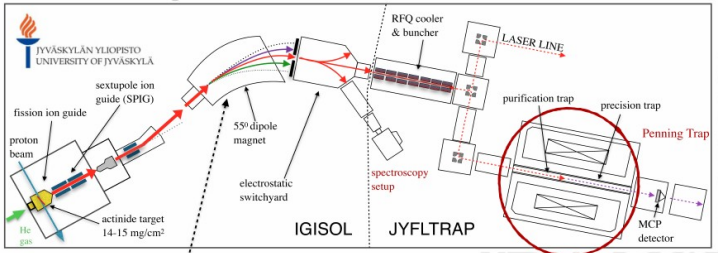
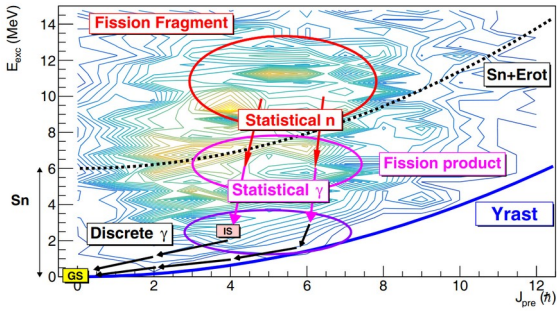
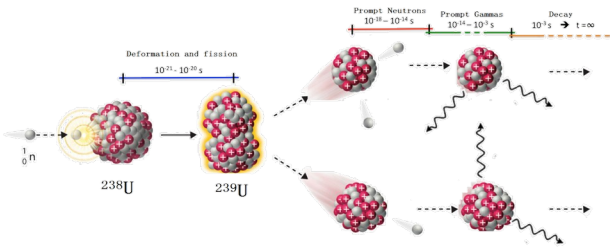
Experimental techniques for measuring isomeric ratios

Results from IGISOL

Linking isomeric yields to fission fragment angular momenta

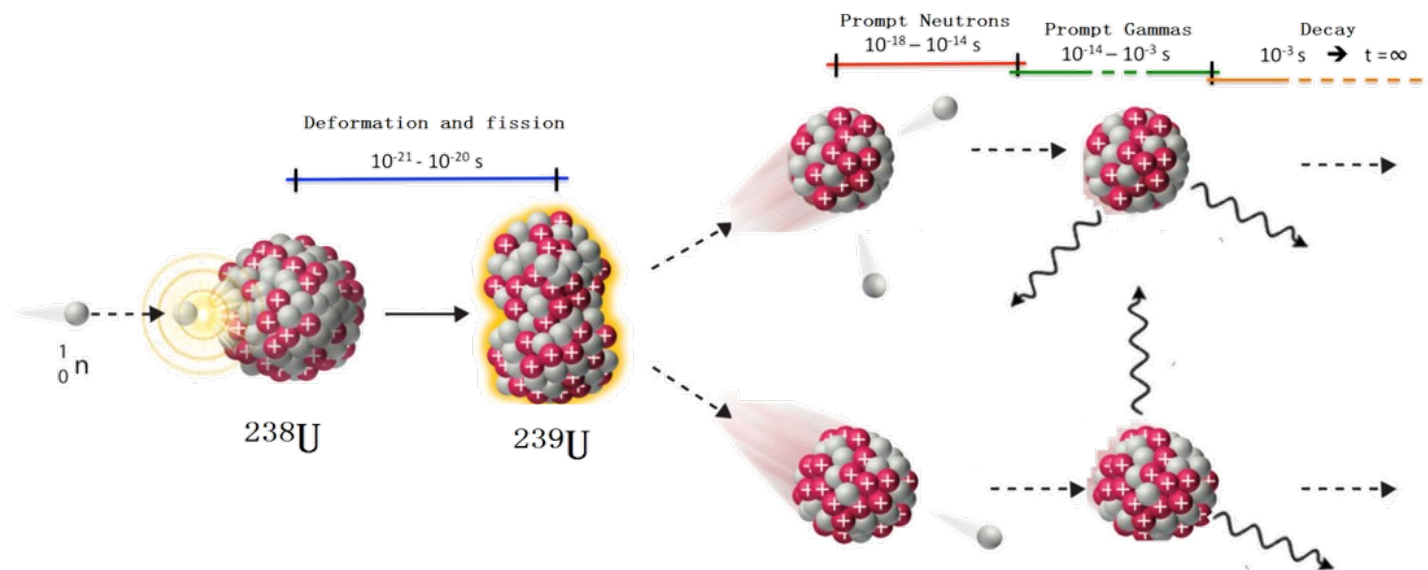
Global comparison of isomeric ratios with model calculations using TALYS

Outlook



UPPSALA  
UNIVERSITET

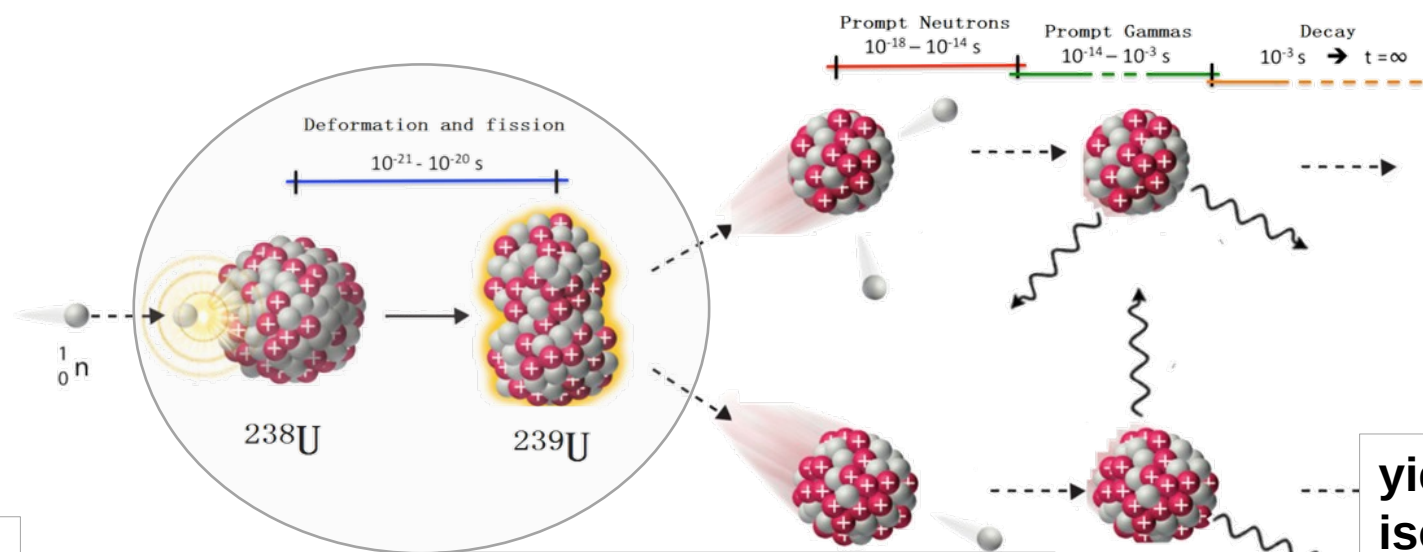
# Fission is the mission



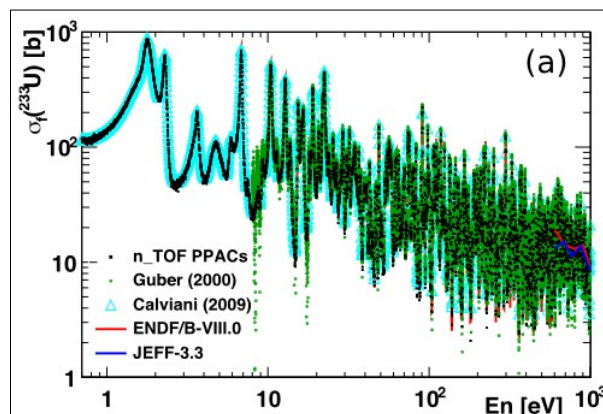
# Fission is the mission



JYVÄSKYLÄN YLIOPISTO  
UNIVERSITY OF JYVÄSKYLÄ

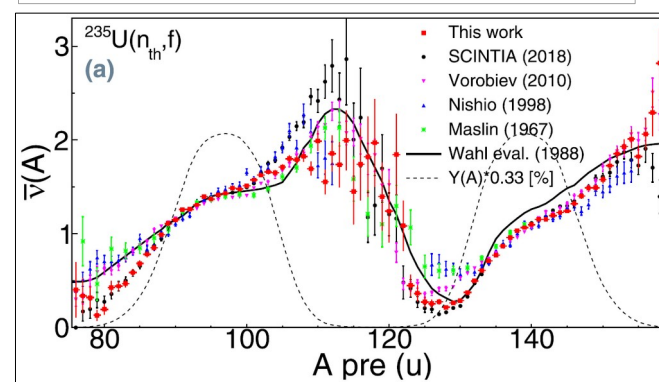


## cross sections



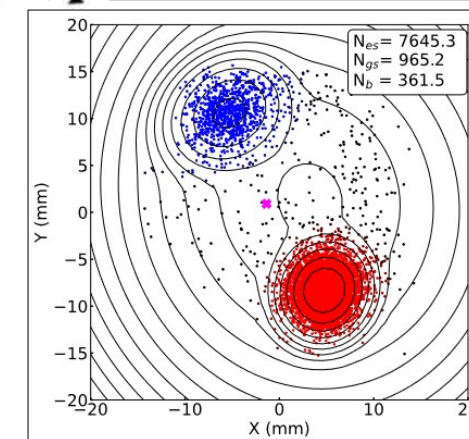
D. Tarrío et al, Phys. Rev. C **107**, 044616 (2023)

## prompt neutron emission



A. Al-Adili et al, Phys. Rev. C **102**, 064610 (2021)

## yields and isomeric ratios



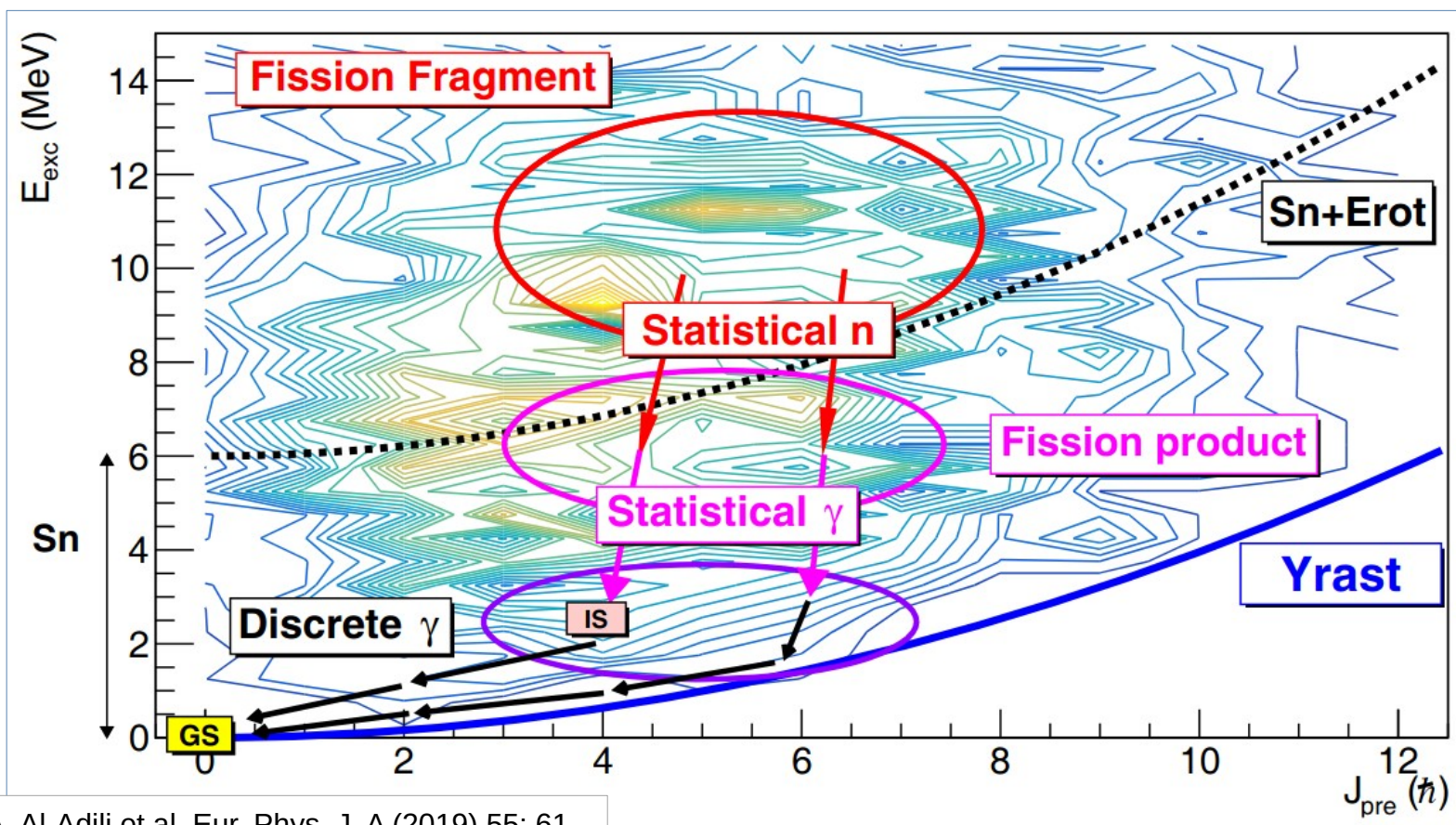
Z. Gao et al, Phys. Rev. C **108**, 054613 (2023)



UPPSALA  
UNIVERSITET



## Population of (isomeric) depends on initial state of the fission fragment



A. Al-Adili et al, Eur. Phys. J. A (2019) 55: 61

Contour plot showing the distribution of excitation energy and spin of the fragments for  $^{136}\text{Xe}$  in  $^{235}\text{U}(n, f)$  as given by GEF 2017.

Basic idea goes back to Huizenga and Vandebosch (1960)

### Our work:

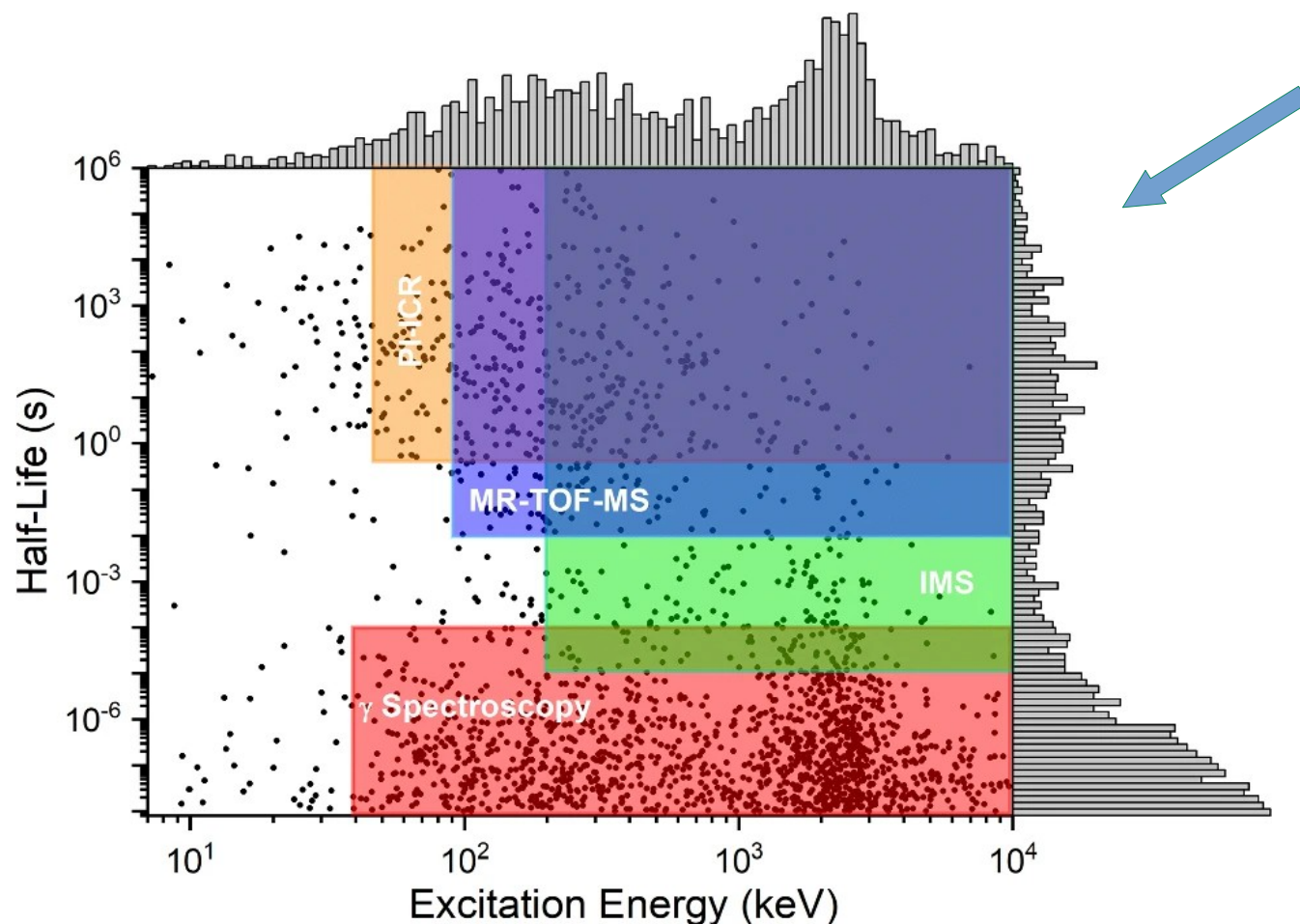
Use experimental measurement data of relative population of (long-lived) isomers, i.e., isomeric yield ratios (IYR), and “back-track”.

$$IYR = \frac{Y_{\text{high spin}}}{Y_{\text{high spin}} + Y_{\text{low spin}}}$$



UPPSALA  
UNIVERSITET

## Possible measurement techniques for IYR



**We use direct ion counting,**  
i.e., mass measurement techniques like  
phase-imaging ion-cyclotron-resonance (PI-ICR)  
and multi-reflection time-of-flight (MR-TOF)

These techniques offer a significant  
advantage compared to techniques using  
 $\gamma$ -ray spectroscopy, since  
we do not rely on available knowledge  
of the nuclear level schemes.

However, these techniques require relatively  
“long” half-lives.

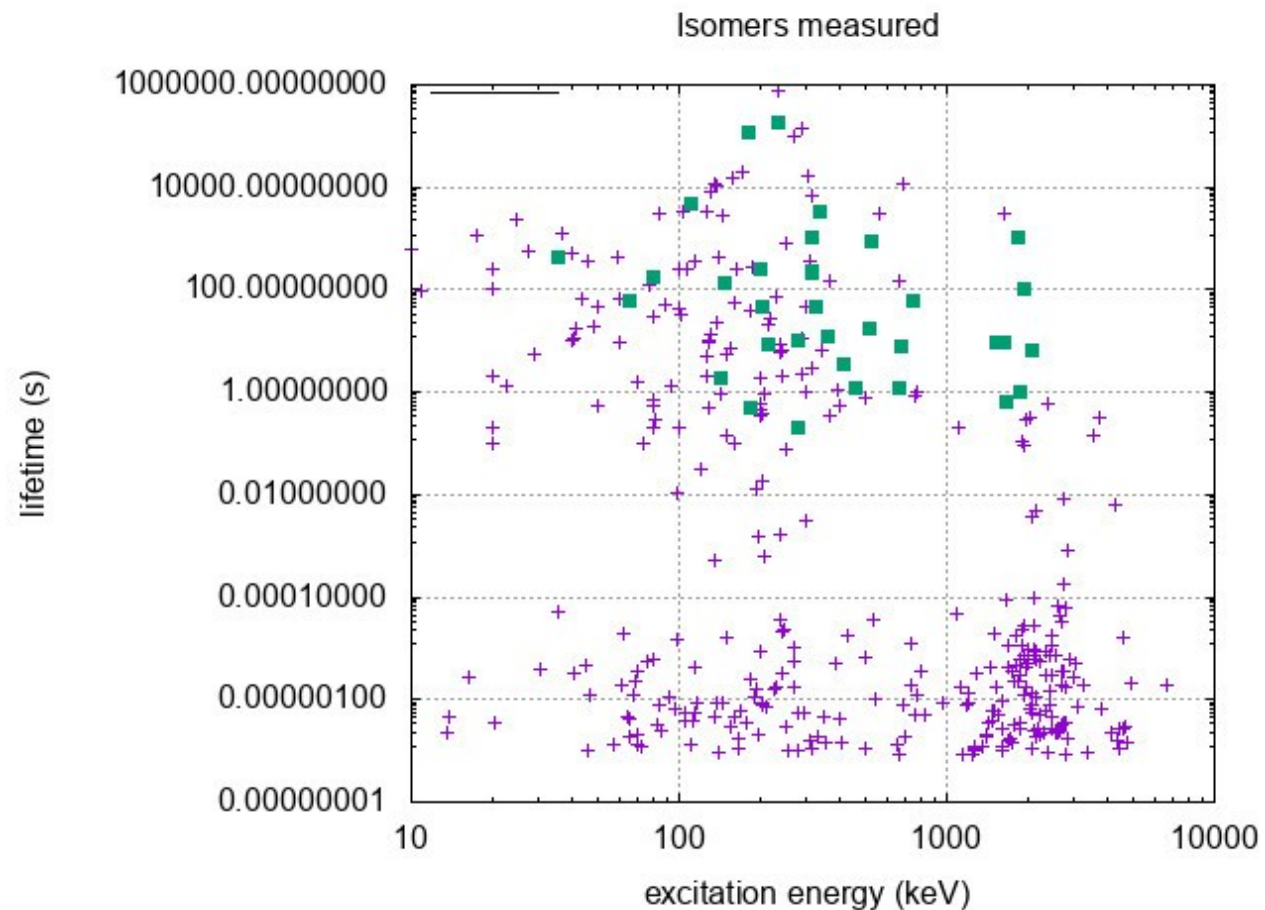
This is pioneered by the Uppsala group in  
collaboration with the IGISOL group  
at the University of Jyväskylä, Finland.

See, e.g., Rakopoulos et al PRC 2018 and 2019,  
and R. Korkiamäki,  
MSc thesis, University of Jyväskylä (2024)



UPPSALA  
UNIVERSITET

## Isomers produced in fission (and IYR we measured with PI-ICR)



Accessible with PI  
and MR-TOF techniques

← 10 ms

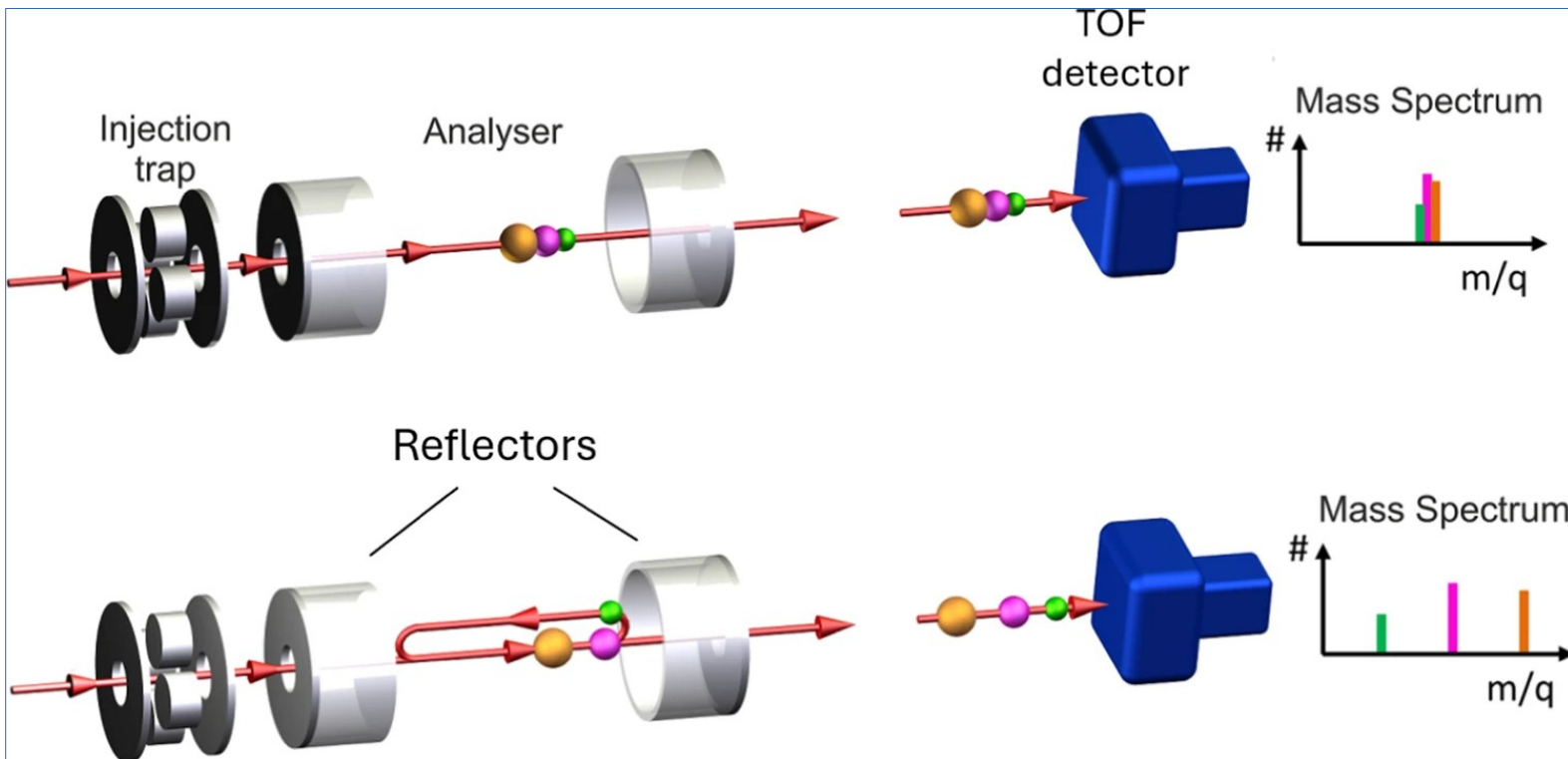
Needs other  
techniques, e.g.,  
gamma spectrometry

The yield is yet another factor of course



UPPSALA  
UNIVERSITET

## Multi-reflection time-of-flight (MR-TOF) - Principle



Injected ions with (the same charge) have a the same kinetic energy and can hence be mass separated by their time-of-flight.

Reflection by electrostatic mirrors increases the flight path.

The mass-resolving power then depends on the number of turns and, e.g., the field stability in the reflectors.

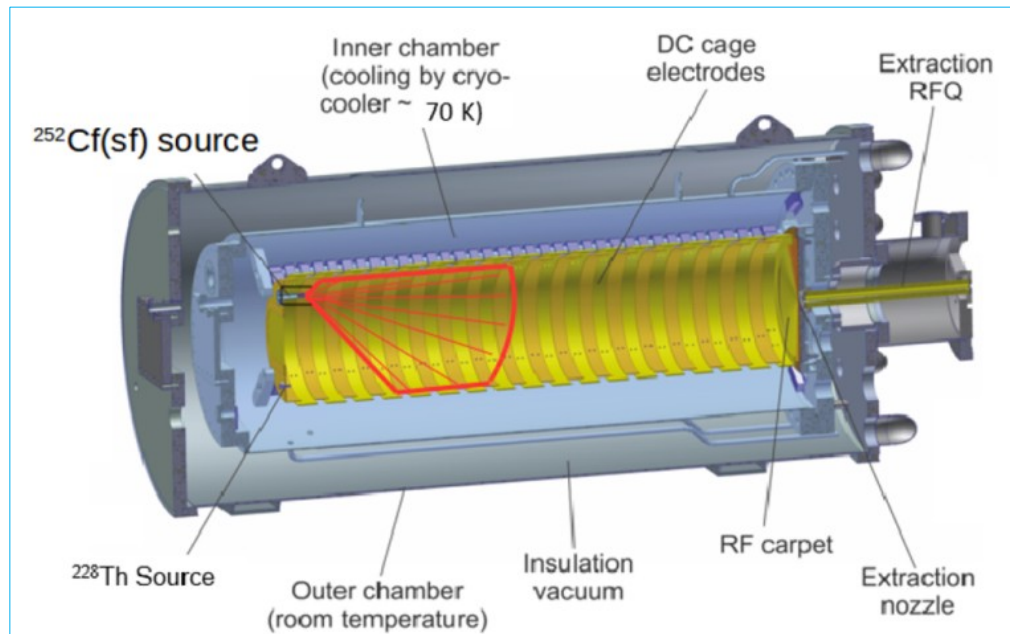
Dickel, T., Mollaebrahimi, A., *Eur. Phys. J. Spec. Top.* **233**, 1181–1190 (2024)



UPPSALA  
UNIVERSITET

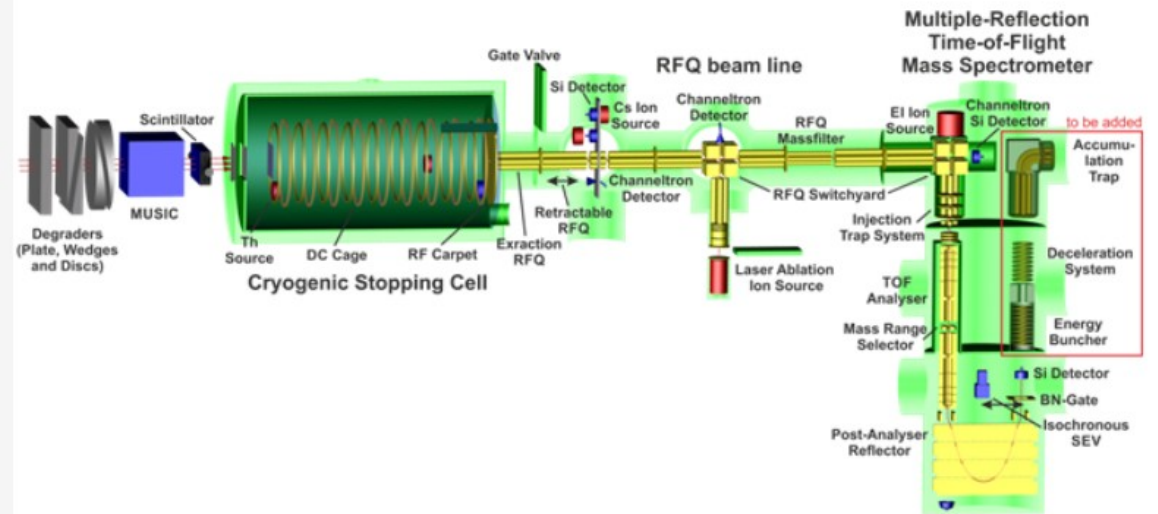


## MR-TOF at CSC @ GSI, Darmstadt

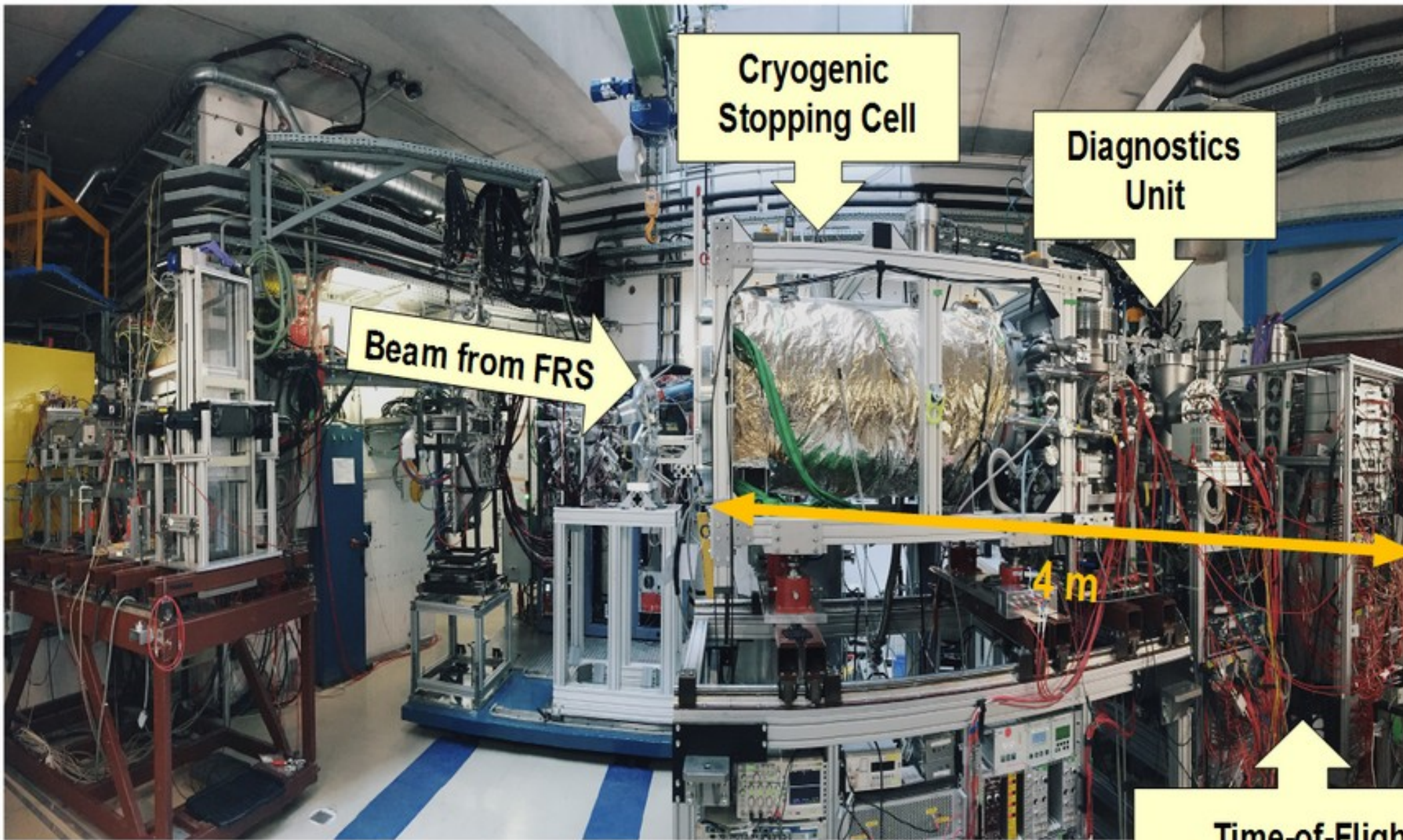


**Figure 1.** Cross section of the CSC with the internal long DC cage that is optimized for thermalizing relativistic ions. The  $^{252}\text{Cf}$  SF source is installed at the upstream side of the CSC, 9 cm off-axis. The red lines mark the approximate range of the emitted FPs in the buffer gas.

Fission product from internal source (or induced via external beam on target) are stopped in the cryogenic stopping cell (CSC) and extracted towards an MR-TOF system.







**Cryogenic  
Stopping Cell**

**Diagnostics  
Unit**

**Beam from FRS**

**4 m**

**Time-of-Flight  
Mass Spectrometer**



UPPSALA  
UNIVERSITET

## MR-TOF at CSC @ GSI, Darmstadt

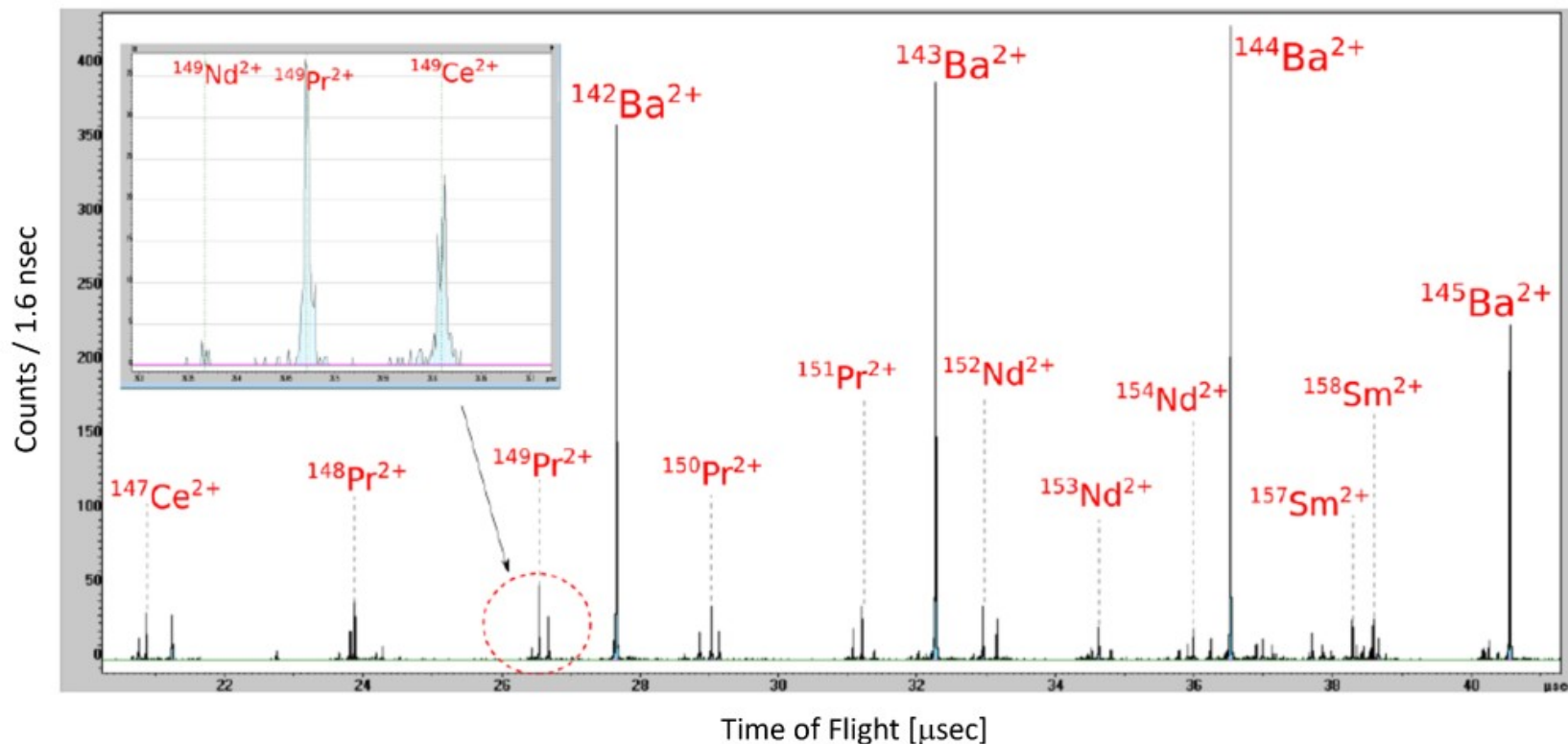


**Figure 2.** Typical time-of-flight spectrum during this experiment. All identified FPs are doubly charged and marked on the plot. The MRP is 320,000. The inset shows the clear separation between three  $A=149$  isobars.

Data from a recent measurement of  $^{252}\text{Cf}(\text{sf})$ .

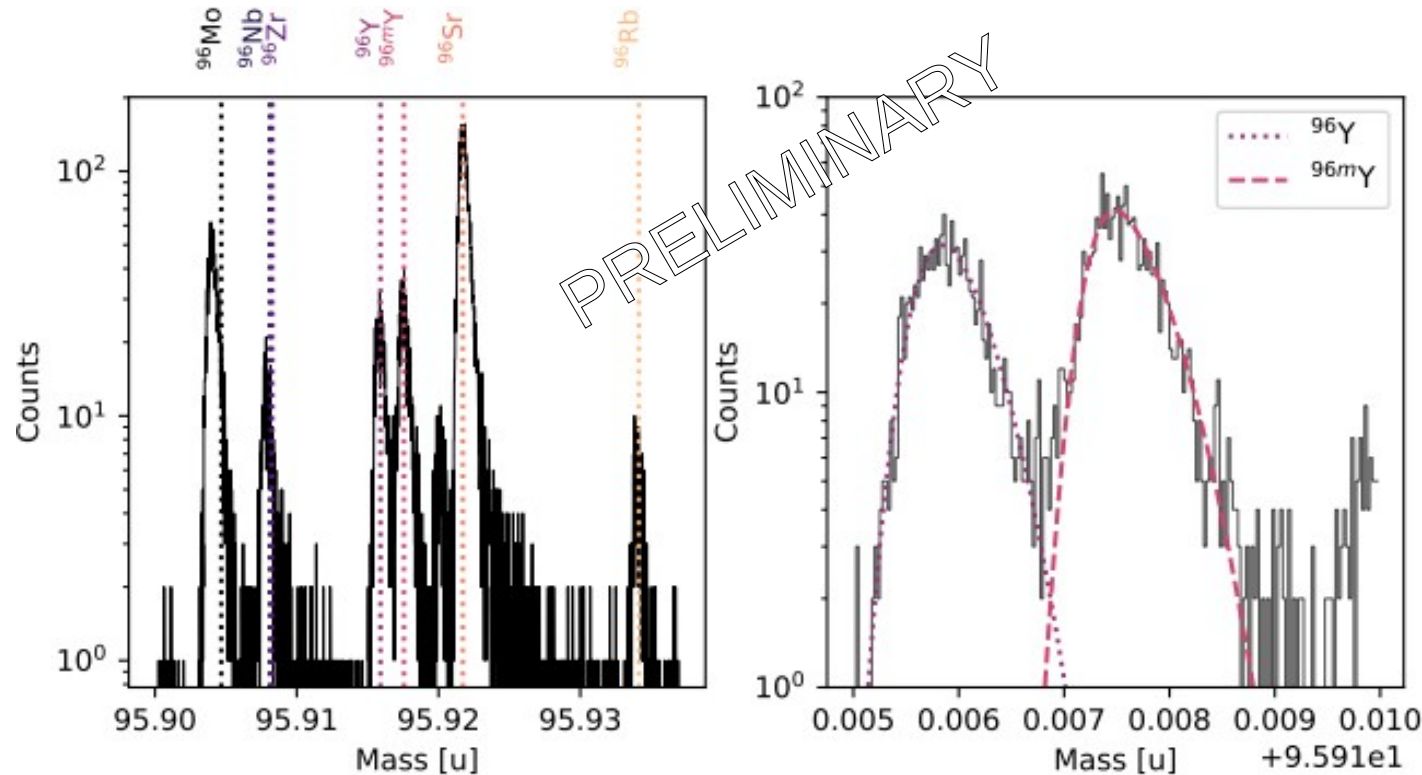
Mass resolving power: 320 000.  
(still less than PI-ICR)

But: MR-TOF systems have achieved  $10^6$  in MRP.

Advantage vs. Penning Trap:  
Extraction from gas cell similar  
but mass measurement much  
faster ( $< \text{ms}$ ).



## Raw data for $^{96}\text{Y}$ from the MR-TOF at IGISOL



Data from a 2023 measurement using  $^{232}\text{Th}(\alpha, f)$  at 28 MeV.

Mass difference between the isomers:  $1.54 \text{ MeV}/c^2$

g.s.:  $0^-$ , ex.s.:  $8^+$

IYR  $\approx 0.59 (\pm 0.02)$  [still prelim.]

(one challenge: understanding the shape of the peaks in the spectrum)

From a paper currently in manuscript



UPPSALA  
UNIVERSITET

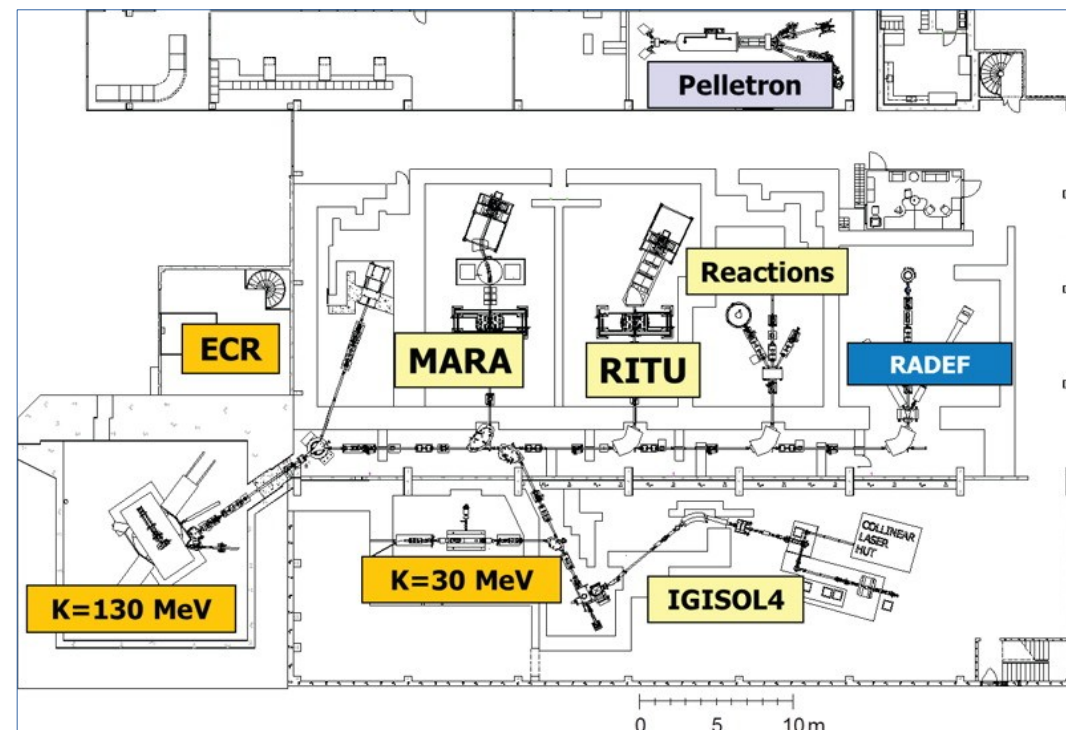
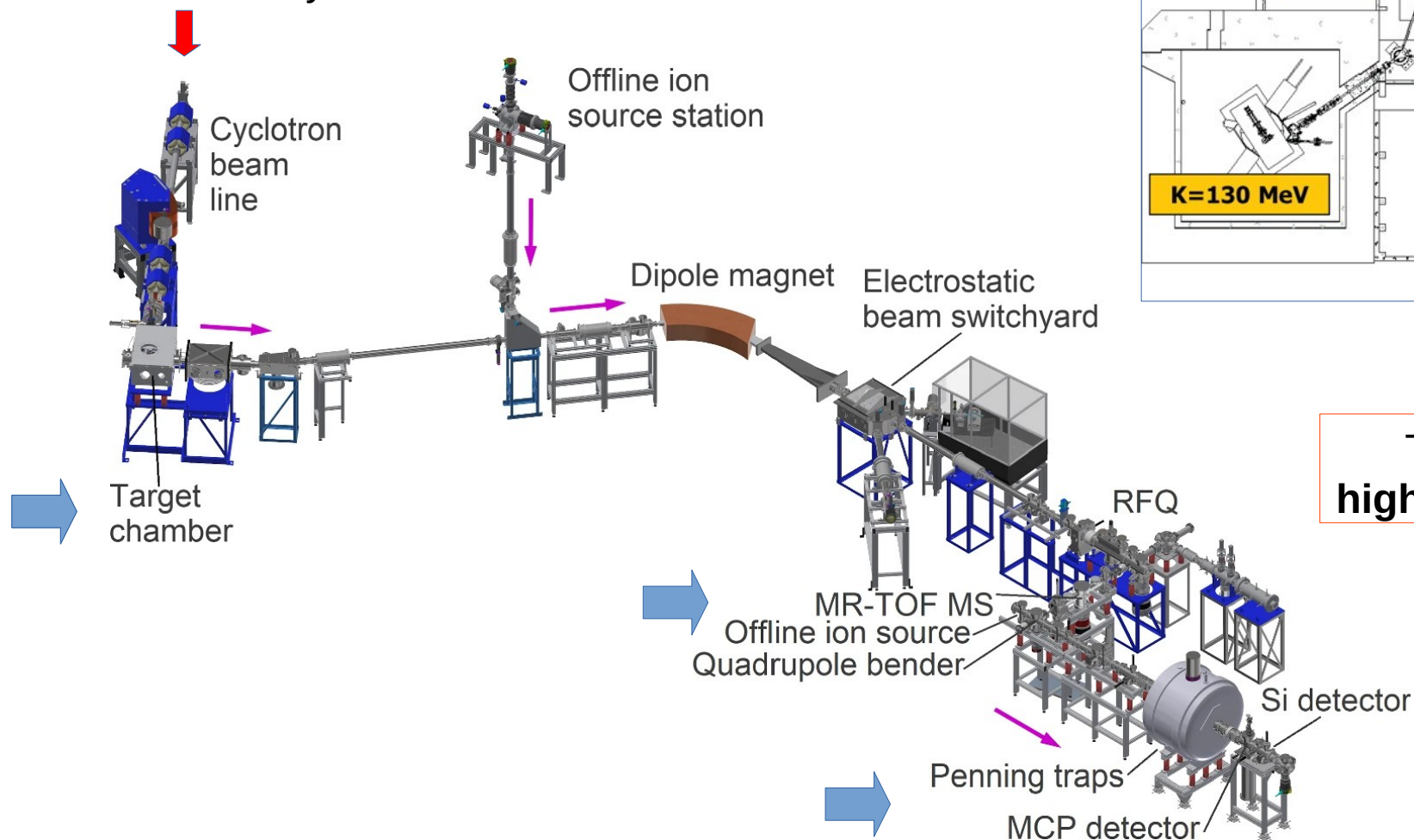


Let's go to Jyväskylä in Finland! [Mennään Jyväskylään Suomessa!]



# IGISOL with MR-TOF and JYFLTRAP

Beam from K-130 cyclotron



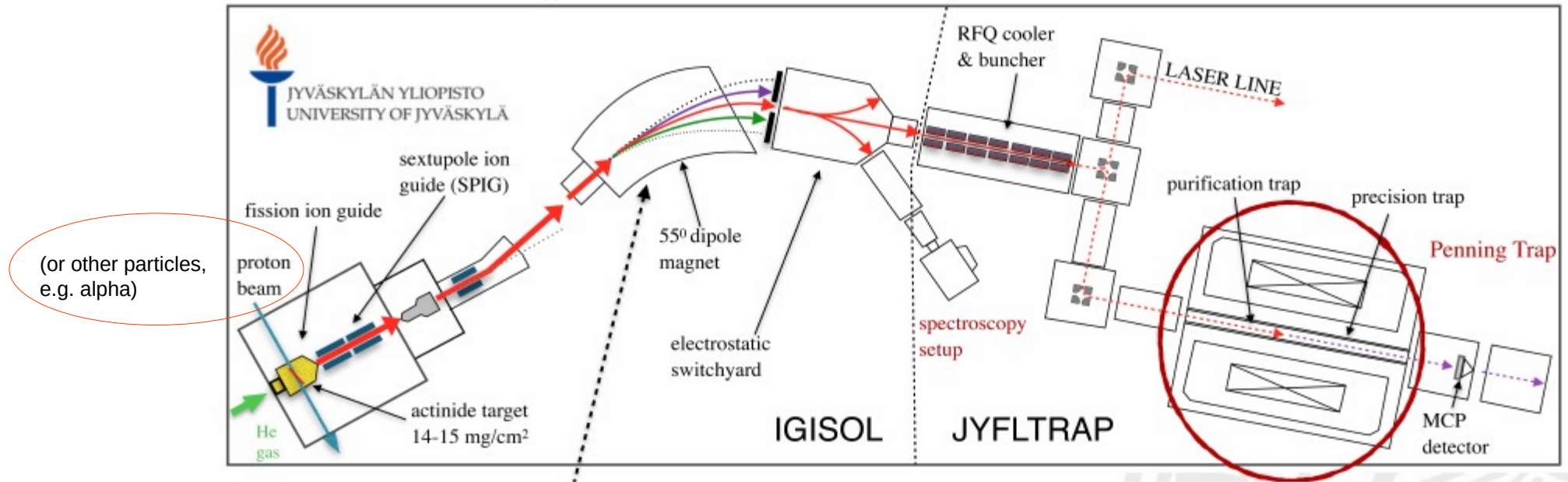
Ari Jokinen, Nuclear Physics News 24(4), 2014  
<https://doi.org/10.1080/10619127.2014.972165>

The lab is well-known for, e.g.,  
**high-precision mass measurements**



UPPSALA  
UNIVERSITET

## IGISOL with MR-TOF and JYFLTRAP



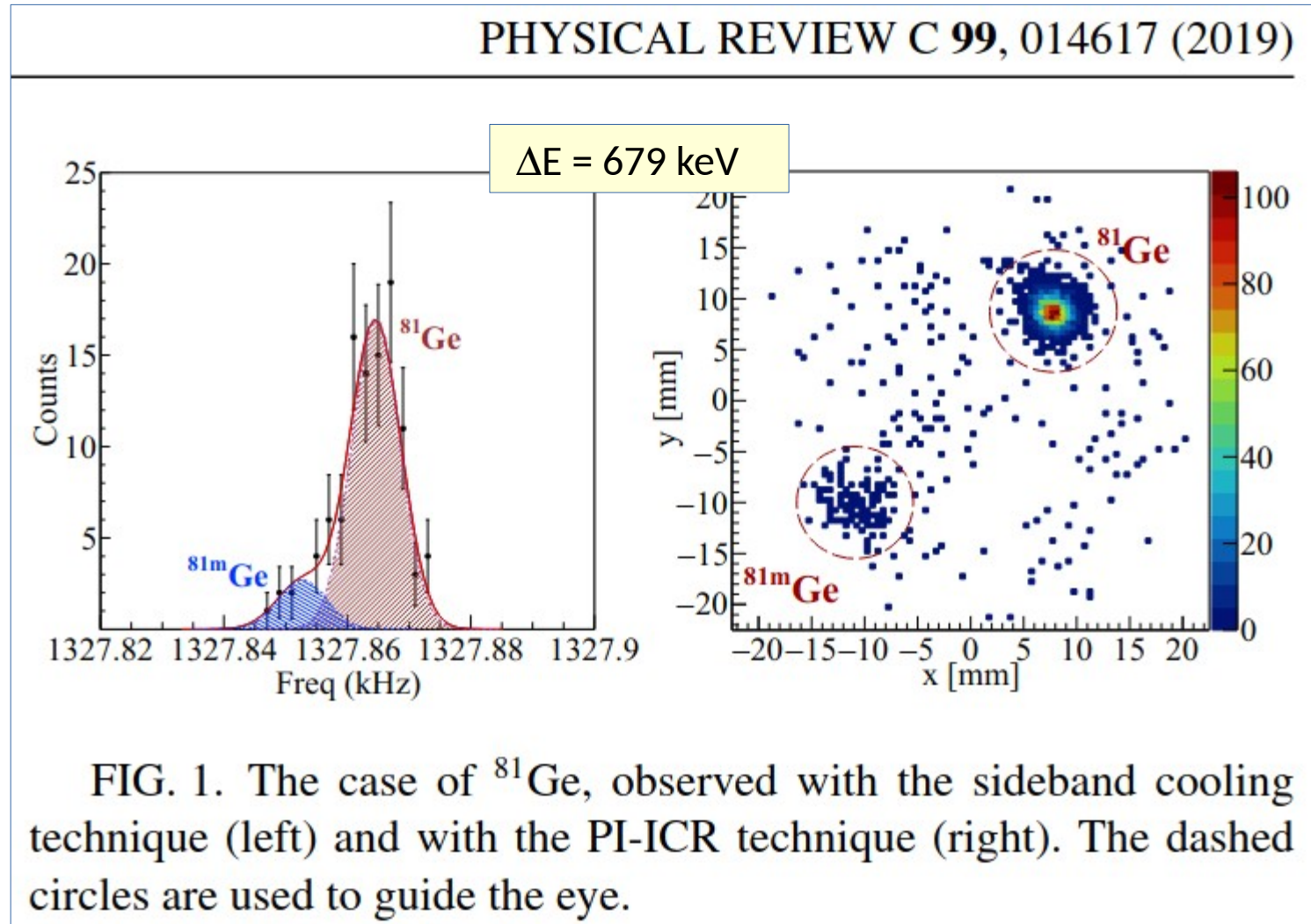
Production of fission fragments – thermalization in helium gas –  
extraction and first mass separation in dipole magnet – cooling and bunching –  
purification and precision trap (double Penning trap JYFLTRAP) – MCP detector

Measurement time (from production to detection): typically 0.5 to 1.5 sec  
**Mass resolving power:**  $> 5 \times 10^6$  (we resolved the 35 keV state in  $^{129}\text{Sn}$ )





The phase-imaging ion-cyclotron-resonance technique (PI-ICR) is powerful!



**PI-ICR:**

S. Eliseev et al.,  
Phys. Rev. Lett. 110, 082501 (2013).

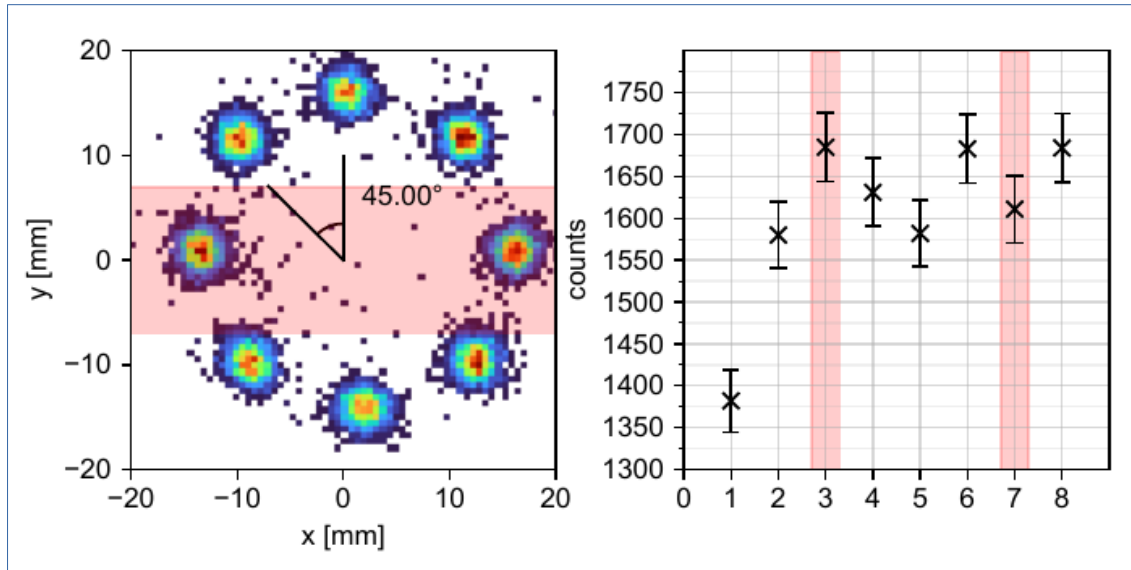


UPPSALA  
UNIVERSITET

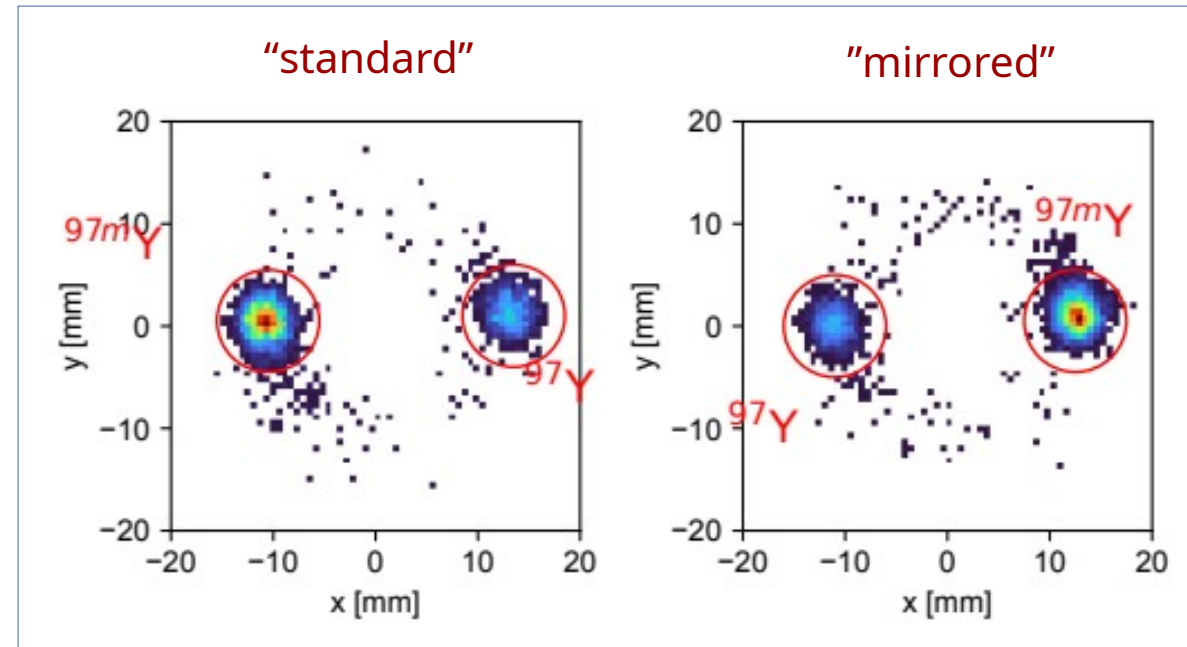


## Main corrections: efficiency of the multi-channel plate (MCP) detector

### Measurement of rel. detection efficiency



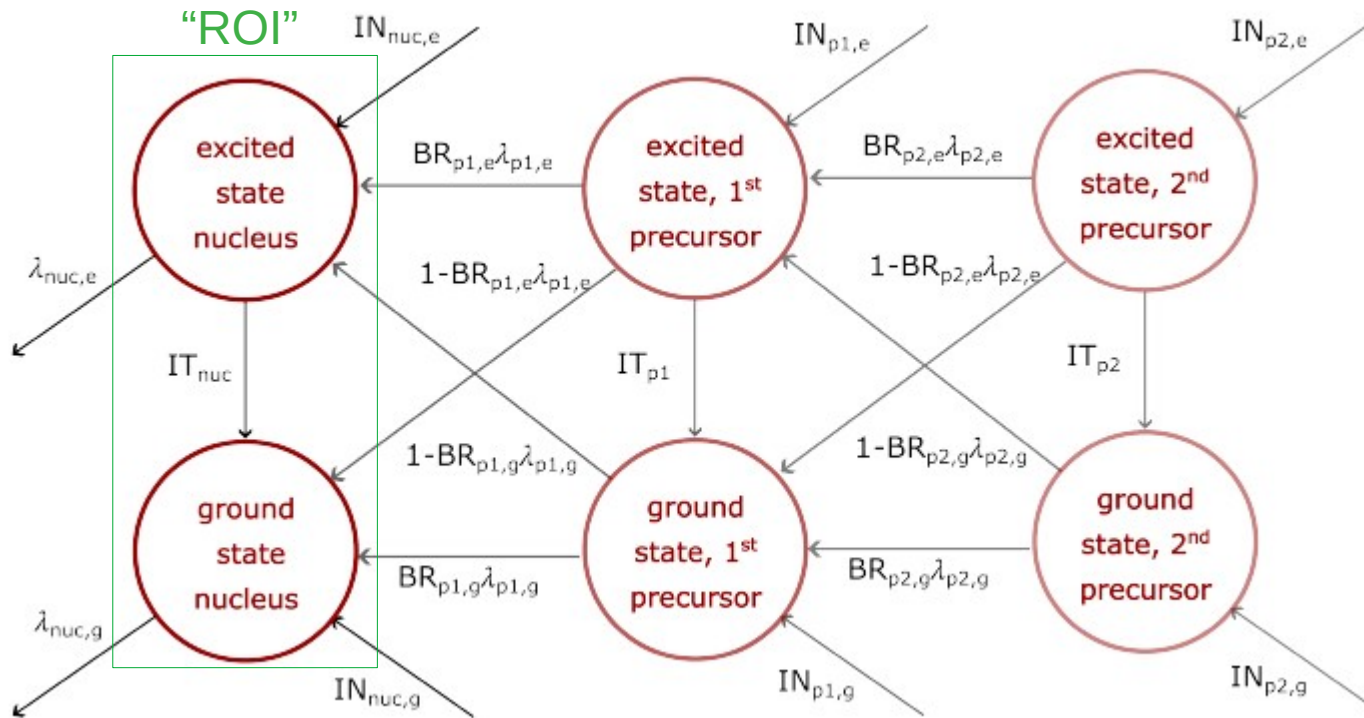
Stable offline ion beam impinges the MCP  
(for same amount of time) at different positions.



Two positions are selected and measurements  
Are repeated with flipped positions of the ion spots  
To cancel out efficiency differences as much as possible.



## Main corrections: decay corrections



We use an iterative procedure with measured ratios as starting guess for true ratio.

Input:

- timing of measurement sequence
- half-lives, branching ratios, relative yields (from ENSDF and GEF).

In most cases this scheme simplifies significantly.

Figure from the licentiate thesis of Simone Cannarozzo.



## Nuclei with IYR data from IGISOL

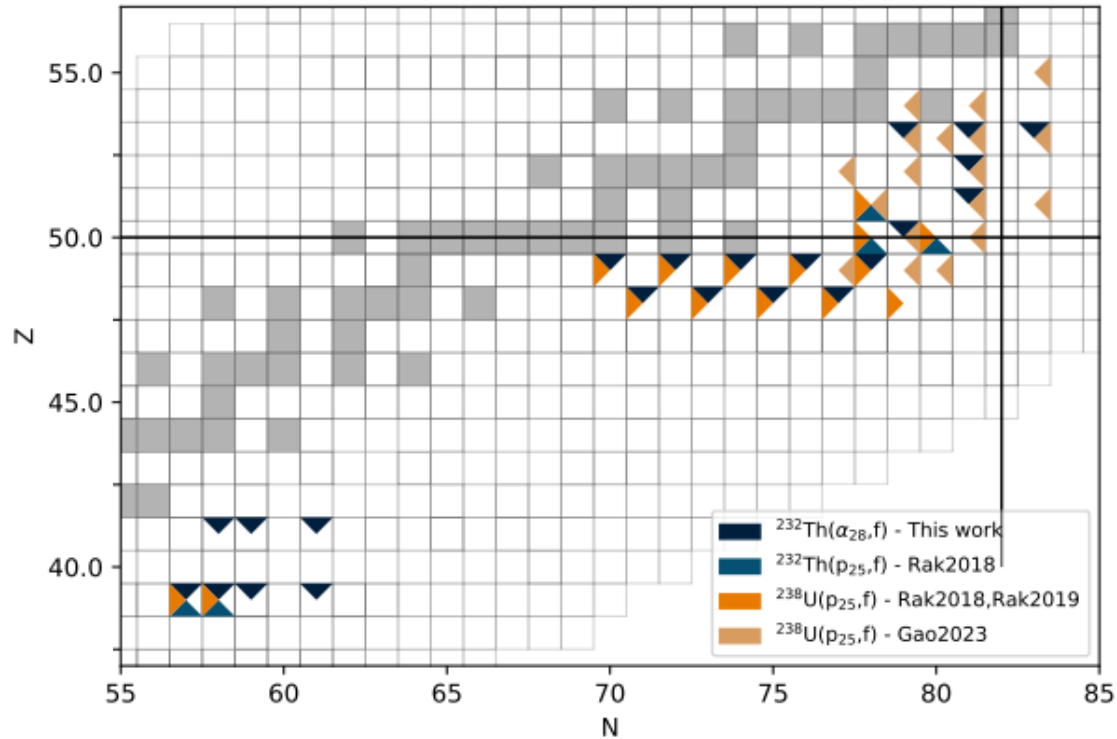


Fig. from S. Cannarozzo thesis (draft)

Several campaigns over the past years using  
 $^{232}\text{Th}(p,f)$  and  $^{238}\text{U}(p,f)$  at 25 MeV (Rakopoulos, Gao)  
 $^{232}\text{Th}(\alpha,f)$  at 28 MeV (Cannarozzo)  
also some data from  
 $^{238}\text{U}(n,f)$  using  $\gamma$ -spectrometry (Mattera)



## Some of our results: $^{238}\text{U}(\text{p},\text{f})$ at 25 MeV

Nuclide	Ground state		Isomeric state			IYR	$J_{\text{rms}}^{\text{av}}$
	$I^\pi$	$T_{1/2}$	$I^\pi$	$T_{1/2}$	$E_x$ (keV)		
$^{81}\text{Ge}$	$9/2^+$ #	8 (2) s	$(1/2^+)$	8 (2) s	679.14(4)	0.975(7)	
$^{119}\text{Cd}$	$1/2^+$	2.69 (2) m	$11/2^-$	2.20 (2) m	146.54(11)	0.871(15)	12.3(5)
$^{121}\text{Cd}$	$3/2^+$	13.5 (3) s	$11/2^-$	8.3 (8) s	214.86(15)	0.867(4)	14.7(1)
$^{123}\text{Cd}$	$3/2^+$	2.10 (2) s	$11/2^-$	1.82 (3) s	143(4)	0.876(7)	15.7(2)
$^{125}\text{Cd}$	$3/2^+$	680 (40) ms	$11/2^-$	480 (30) ms	186(4)	0.902(8)	
$^{127}\text{Cd}$	$3/2^+$	360 (40) ms	$11/2^-$	450 (120) ms	276(15)	0.872(38)	
$^{119}\text{In}$	$9/2^+$	2.4 (1) m	$1/2^-$	18.0 (3) m	311.37(3)	0.978(15)	26.2(4)
$^{121}\text{In}$	$9/2^+$	23.1 (6) s	$1/2^-$	3.88 (10) m	313.68(7)	0.971(11)	25.1(5)
$^{123}\text{In}$	$(9/2)^+$	6.17 (5) s	$(1/2)^-$	47.4 (4) s	327.21(4)	0.958(2)	21.2(2)
$^{125}\text{In}$	$9/2^+$	2.36 (4) s	$(1/2)^{-(-)}$	12.2 (2) s	360.12(9)	0.950(3)	15.9(3)
$^{127}\text{In}$	$(9/2^+)$	1.09 (1) s	$1/2^-$ #	3.67 (4) s	408.9(3)	0.921 (2)	9.5 (2)
			$(21/2^-)$	1.04 (10) s	1870 (60)		
$^{129}\text{Sb}$	$7/2^+$	4.366 (26) h	$(19/2^-)$	17.7 (1) m	1851.31(6)	0.441(32)	

V. Rakopoulos et al., Phys. Rev. C **99**, 014617 (2019)

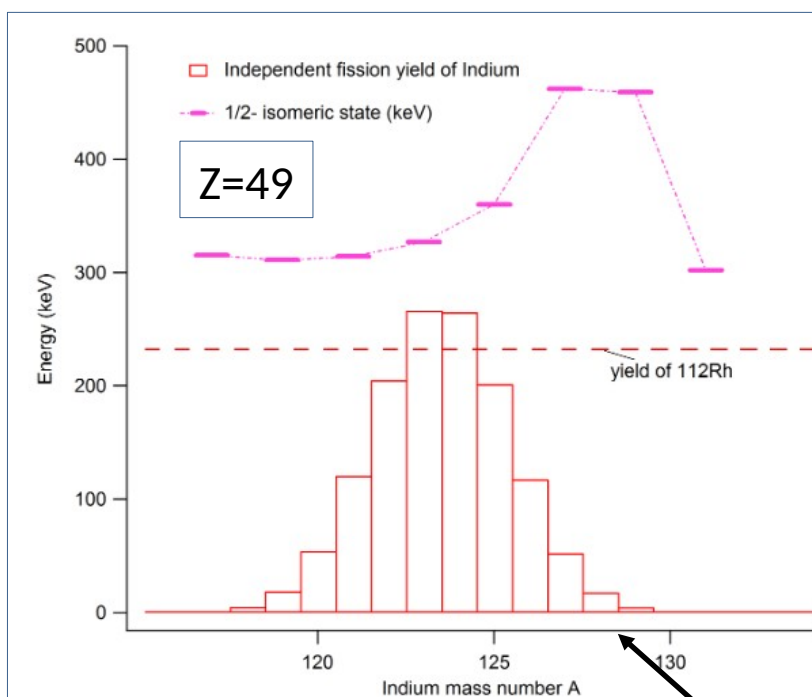




Some of our results:  $^{238}\text{U}(\text{p},\text{f})$  at 25 MeV – focus on Cd and In

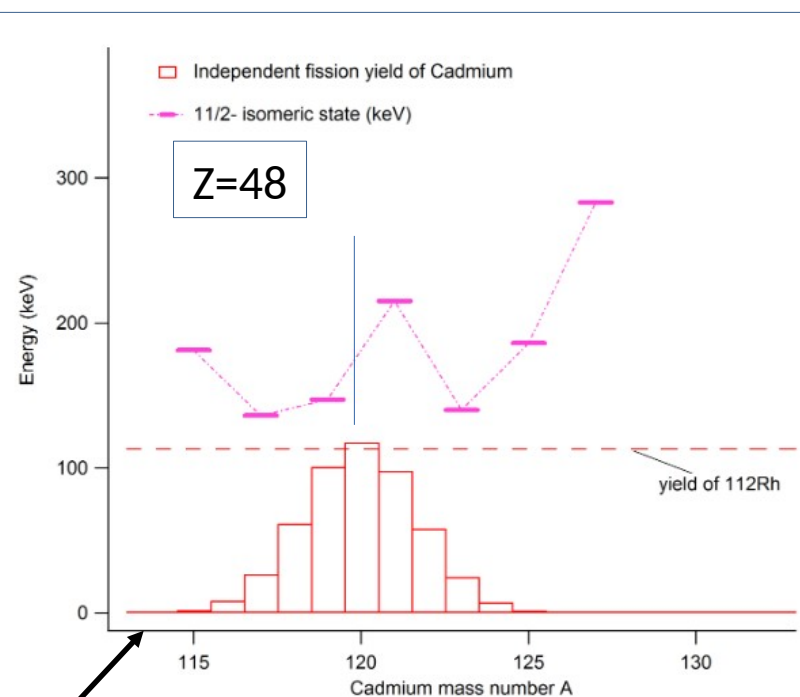
In

Proton hole in  $1g_{9/2}$  resp  $2p_{1/2}$



Cd

Neutron hole in  $3s_{1/2}/2d_{3/2}$  resp  $1h_{11/2}$



IFY according to H. Penttilä et al., Eur. Phys. J. A **52**:104 (2016).



UPPSALA  
UNIVERSITET

## Some of our results: $^{238}\text{U}(p,f)$ at 25 MeV – focus on Cd and In

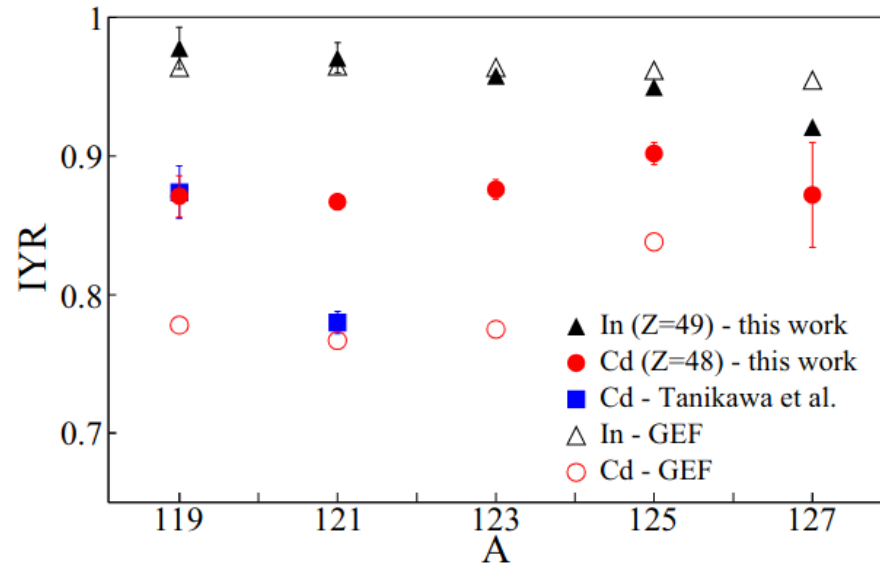


FIG. 3. The experimentally determined isomeric yield ratios for the isotopes of In and Cd as measured in this work by employing the PI-ICR technique. The data are compared with data available in the literature [72], and with results from calculations performed with the GEF model [70,71]. The error bars in the experimental results are smaller than the data points, whenever they are not visible in the figure.

V. Rakopoulos et al., Phys. Rev. C **99**, 014617 (2019)

Results from our first campaign using PI-ICR at IGISOL.

Focus was on Cd and In isomeric pairs.

All **Cd**:  $3/2^+$  and  $11/2^-$  (except  $^{119}\text{Cd}$ )

All **In**:  $9/2^+$  and  $1/2^-$

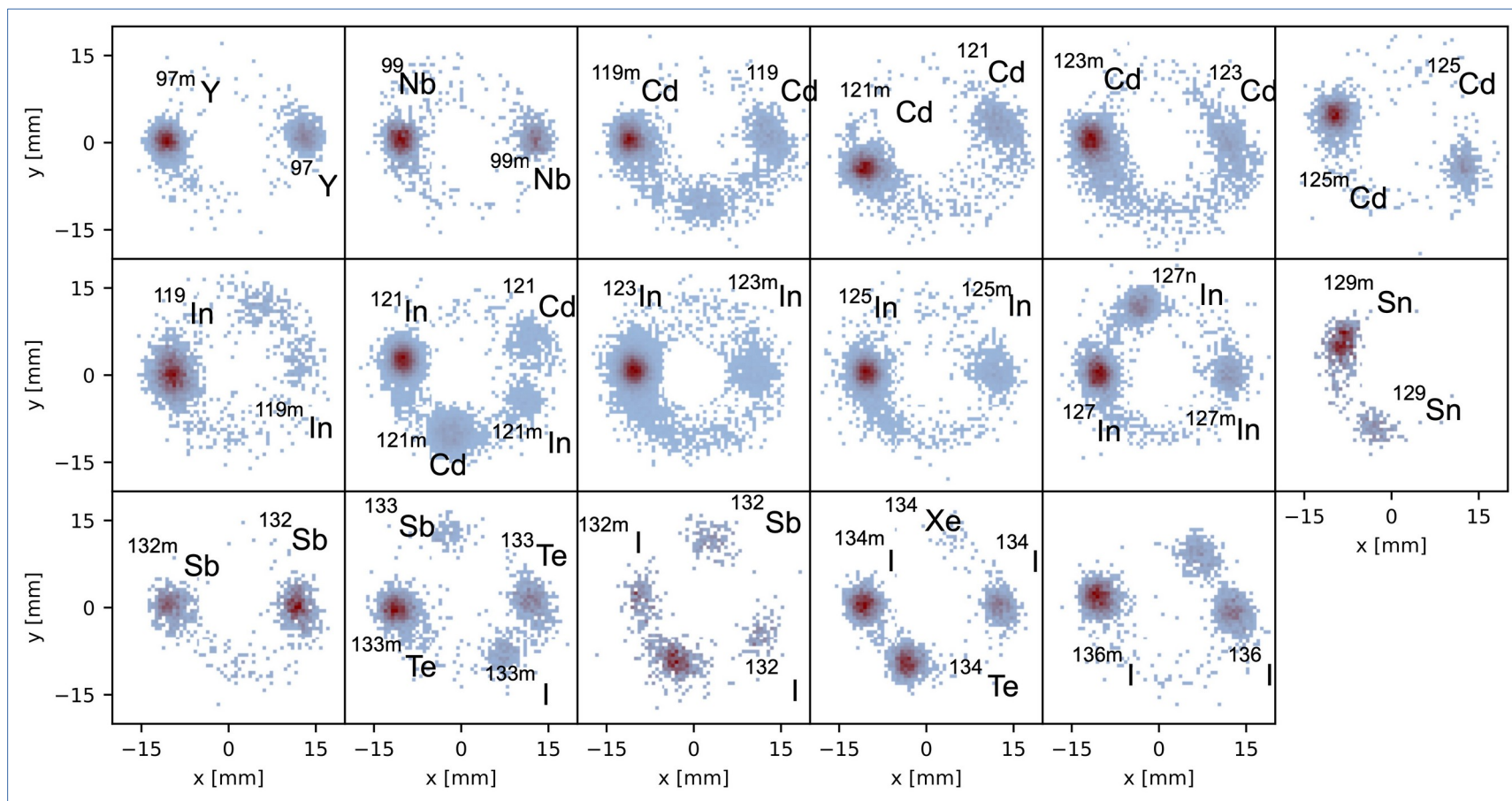
i.e.  $\Delta J = 4 \hbar$  in (almost) all cases.

The successful measurement and the observed trends (especially in In) motivated extension of our measurements to further cases.



UPPSALA  
UNIVERSITET

## Some of our results: $^{232}\text{Th}(\alpha, f)$ at 28 MeV



Why  $^{232}\text{Th}(\alpha, f)$ ?

Induce large CN spin.

Impact on IYR?

Compare to  $^{233,235}\text{U}(n_{th}, f)$ .

We find that a significant part  
(at least 40%)  
of the extra CN spin  
goes to the FF  
(rest to orbital ang. momentum)

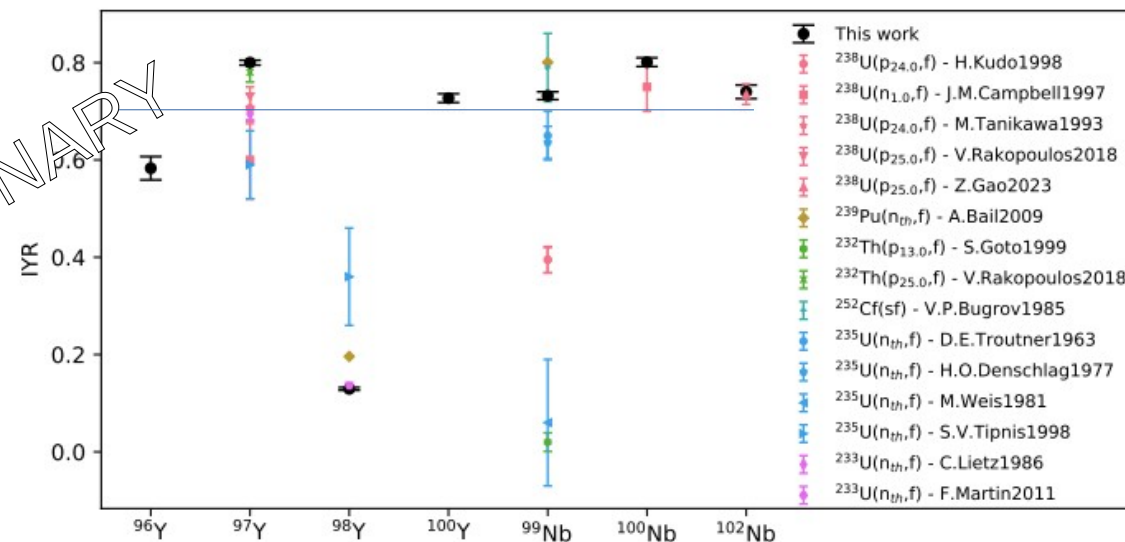
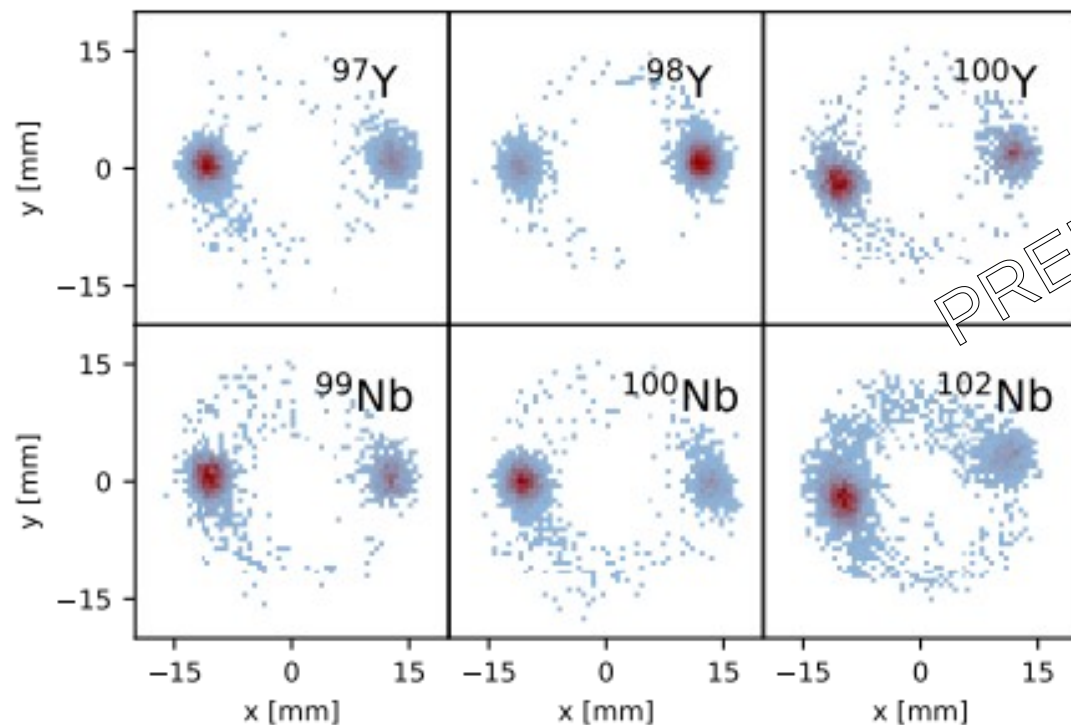
<https://arxiv.org/abs/2412.04340>

Accepted for publication as a Letter in PRC



UPPSALA  
UNIVERSITET

## The peculiar case of $^{98}\text{Y}$



Outlier – reason?

$^{98}\text{Y}$  known for large isomeric shift

But how to explain?

Spin assignment experimentally verified!

From a paper currently in manuscript



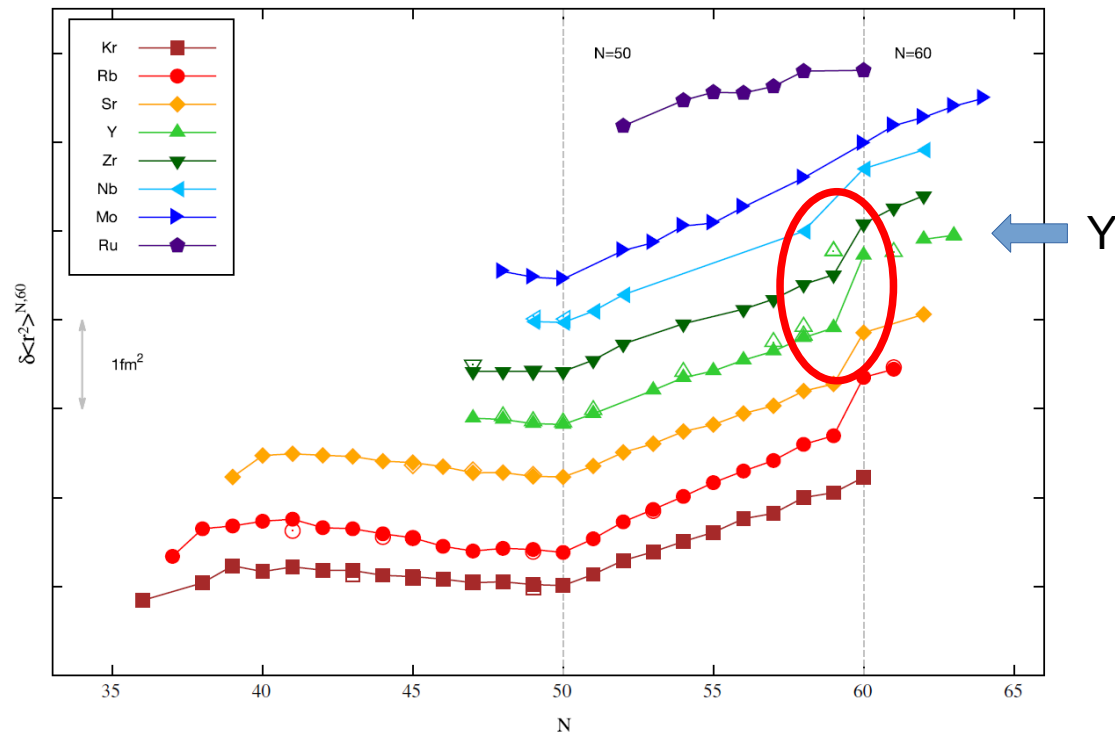
UPPSALA  
UNIVERSITET



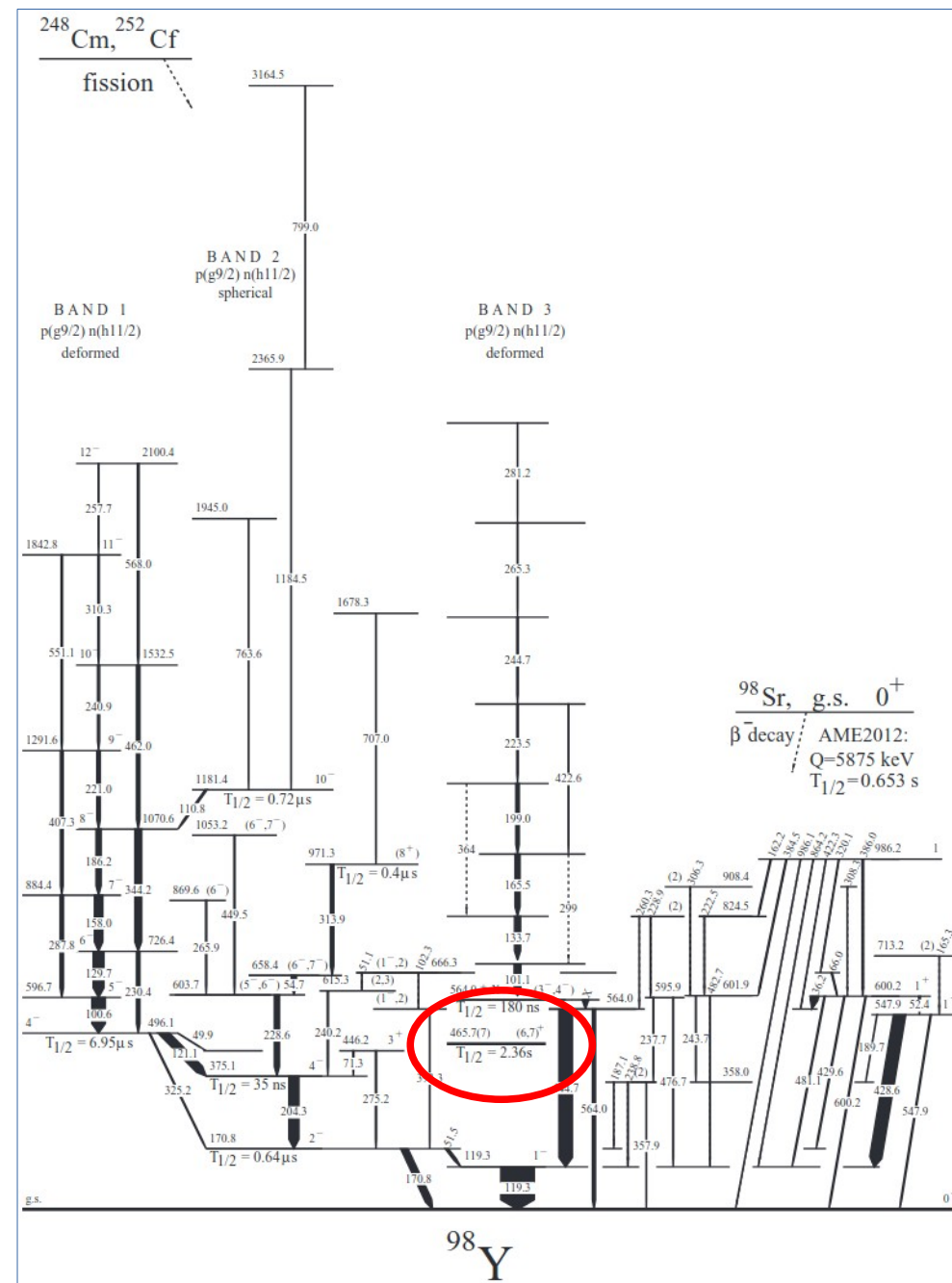
# The peculiar case of $^{98}\text{Y}$

162

P. Campbell et al. / Progress in Particle and Nuclear Physics 86 (2016) 127–180

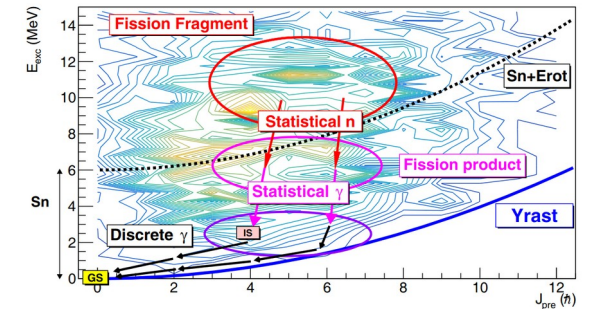
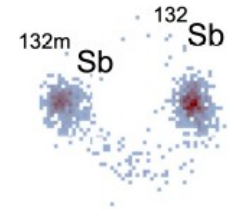


- $^{98}\text{Y}$  shows a large isomeric shift (also  $^{79}\text{Zn}$ )
- Shape co-existence
- Isomer rarely populated in fission



All nice and good ...  
... so now what do we do with these data?

- Nuclear structure data are not needed to obtain IYR by direct ion counting  
(with the exception of data needed for decay corrections)
- But we actually want to know something about the state of the fission fragment
- Need nuclear structure data and nuclear level densities to model de-excitation



## First attempt: Use TALYS and a trial-and-error procedure

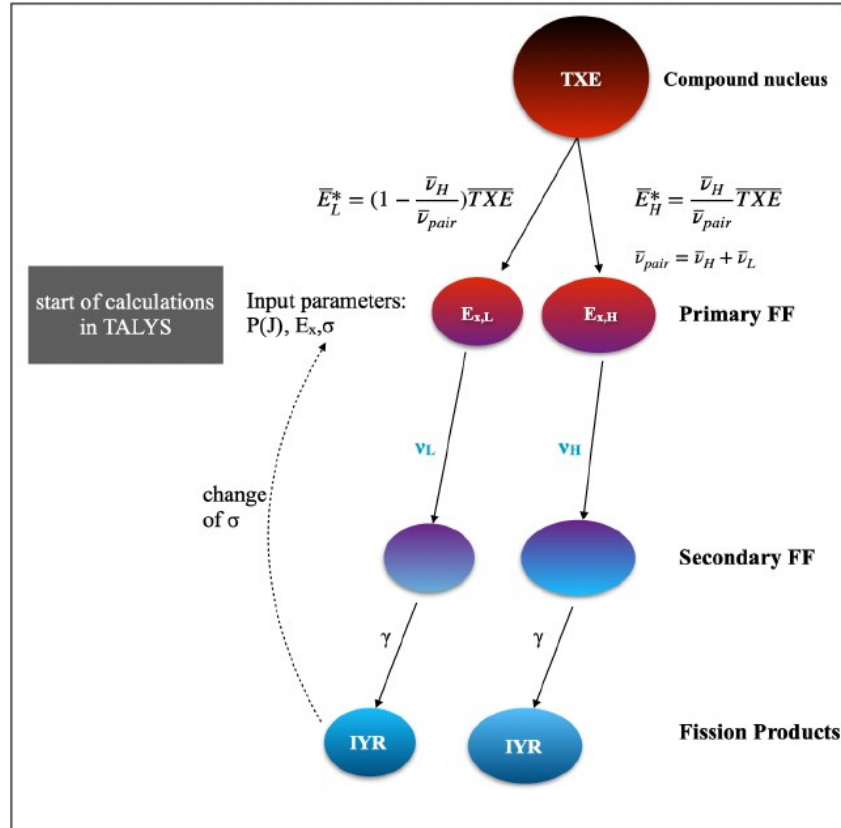
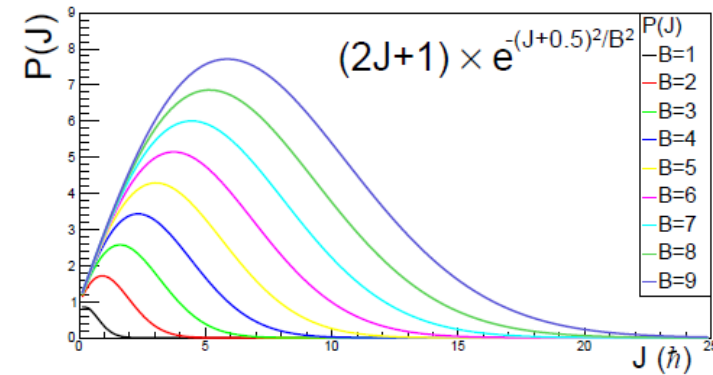


Figure 6.1. Schematic overview of the methodology for the estimation of the isomeric yield ratio by employing the reaction code TALYS. From the intersection between the experimentally determined yield ratio and the one estimated by TALYS, the root-mean-square angular momentum ( $J_{rms}$ ) of the primary fragments can be derived.

V. Rakopoulos, PhD thesis, Uppsala 2019

← Average TXE as given by GEF

← Simple model for sharing of TXE using multiplicities from Rubchenya (<sup>nat</sup>U) and Isaev (<sup>232</sup>Th)



Probability distribution for total angular momentum of the fragments

$$J_{rms} = \sqrt{\bar{J}^2 + \text{Var}(J)}.$$



UPPSALA  
UNIVERSITET

# First steps

FIRST ISOMERIC YIELD RATIO MEASUREMENTS BY ...

PHYSICAL REVIEW C **98**, 024612 (2018)

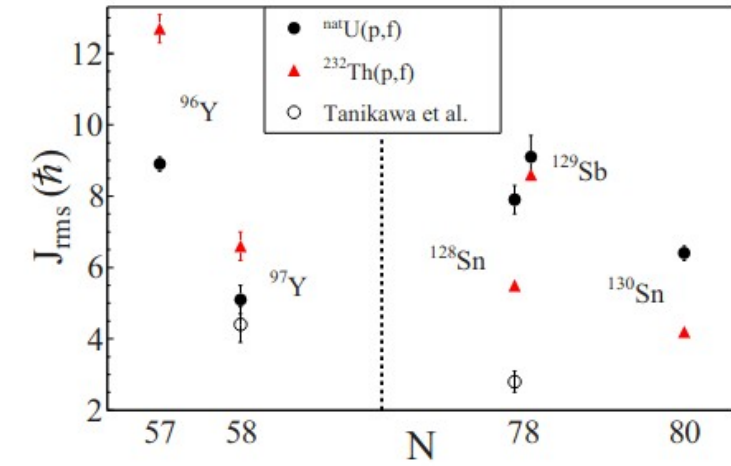
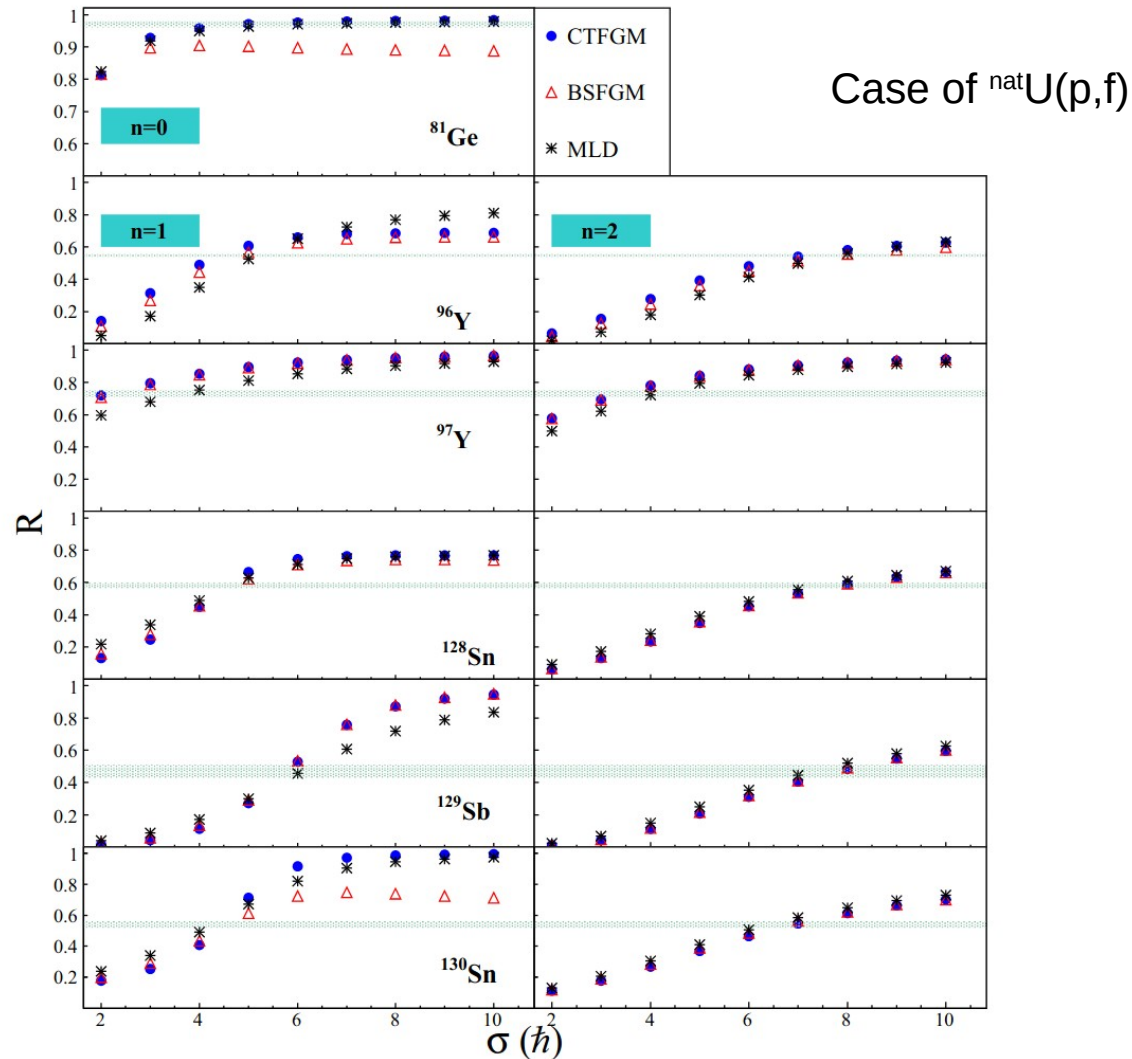


FIG. 9. The deduced  $J_{\text{rms}}$  for the two fissioning systems as a function of the neutron number of the fission products.

Very simplistic approach (the experimentalist way):

Start 0,1 or 2 neutrons away from product

Calculate starting conditions (energy sharing)

Let TALYS do it's job

Weigh results and get a guess for  $J_{\text{rms}}$



UPPSALA  
UNIVERSITET



## First steps – it does not always work

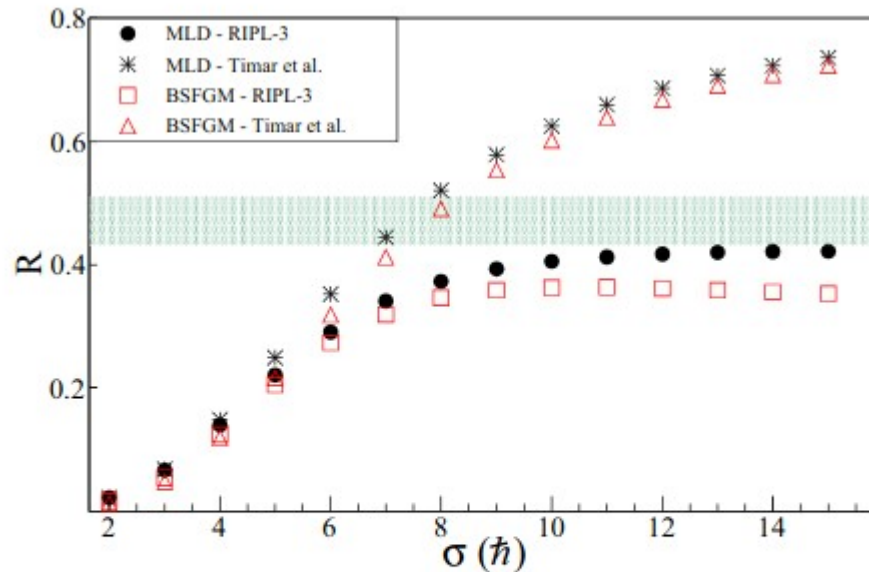


FIG. 8. The case of  $^{129}\text{Sb}$ , where the calculations were performed with the level scheme of RIPL-3 and the updated level scheme from Ref. [88]. In red, the results for the BSFGM and in black for the MLD model.

$^{129}\text{Sb}$  was an interesting case:

We could not reproduce the IYR at all

Add new nuclear structure data  
(to what is in RIPL-3) from Timar et al. ...

... and we can find a solution.



## Same principle but using GEF to produce distribution of starting points ...

Two cases where “all” agree:

Test of method.  
Not our IYR data.

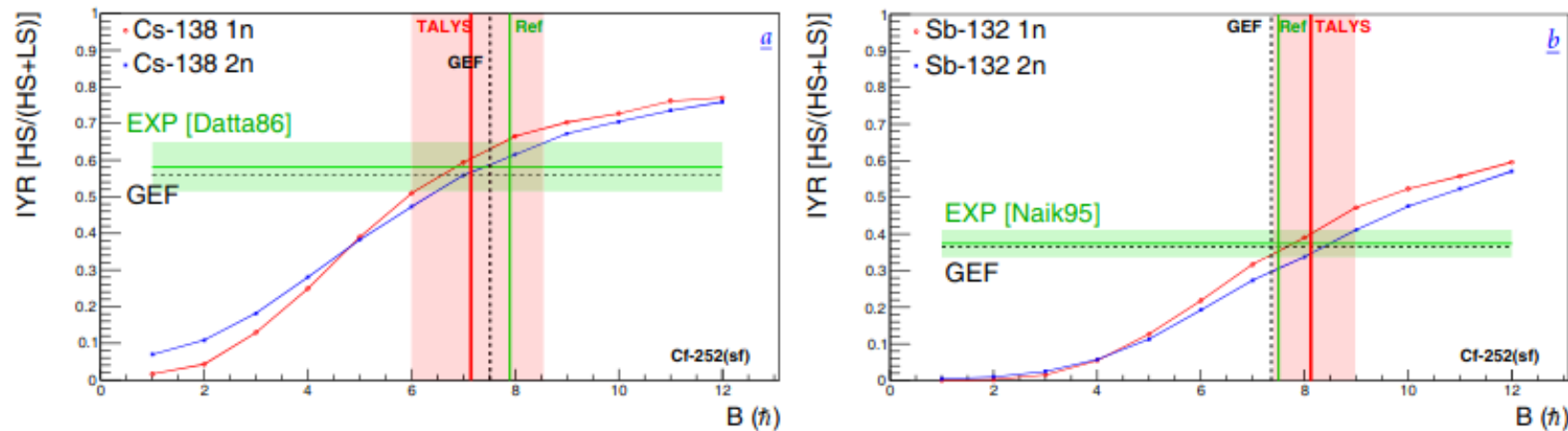


**Fig. 4.** Two examples where a perfect match between TALYS, GEF and literature [17,6] could be achieved. The vertical lines show  $B$  as extracted from GEF (dashed black line), TALYS (full thick red line) and the experiment (full green line). (a) The calculations for Cs-138 assuming 1 (red circles) or 2 (blue squares) neutrons emitted. All three data-sets agree in this case pointing to a  $J_{\text{rms}} \approx 7-8\hbar$ . (b) The calculations for Sb-132 which give a  $J_{\text{rms}} \approx 7-8\hbar$ .

## Same principle but using GEF to produce distribution of starting points ...

Two cases which differ from value given in the original publication:

Test of method.  
Not our IYR data.

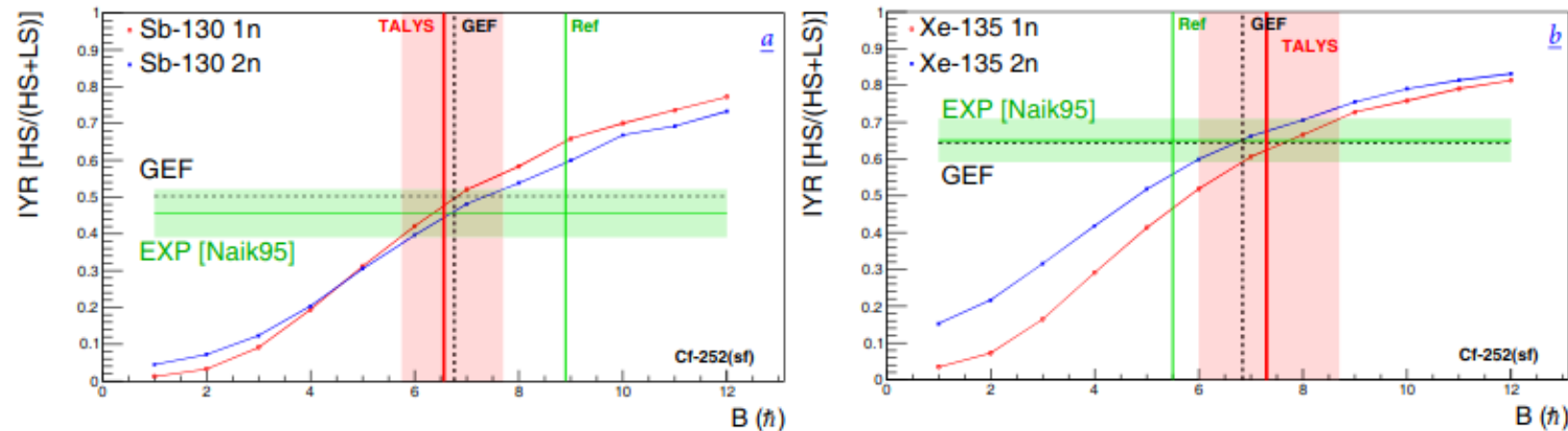


**Fig. 5.** Two examples where both GEF and TALYS disagree with literature data [6]. The vertical lines show  $B$  as extracted from GEF (dashed black line), TALYS (full thick red line) and the experiment (full green line). (a) The calculations for Sb-130 assuming 1 (red circles) or 2 (blue squares) neutron emissions separately. (b) The calculations for Xe-135.

Same principle but using GEF to produce distribution of starting points ...

Two cases problematic cases:

Test of method.  
Not our IYR data.

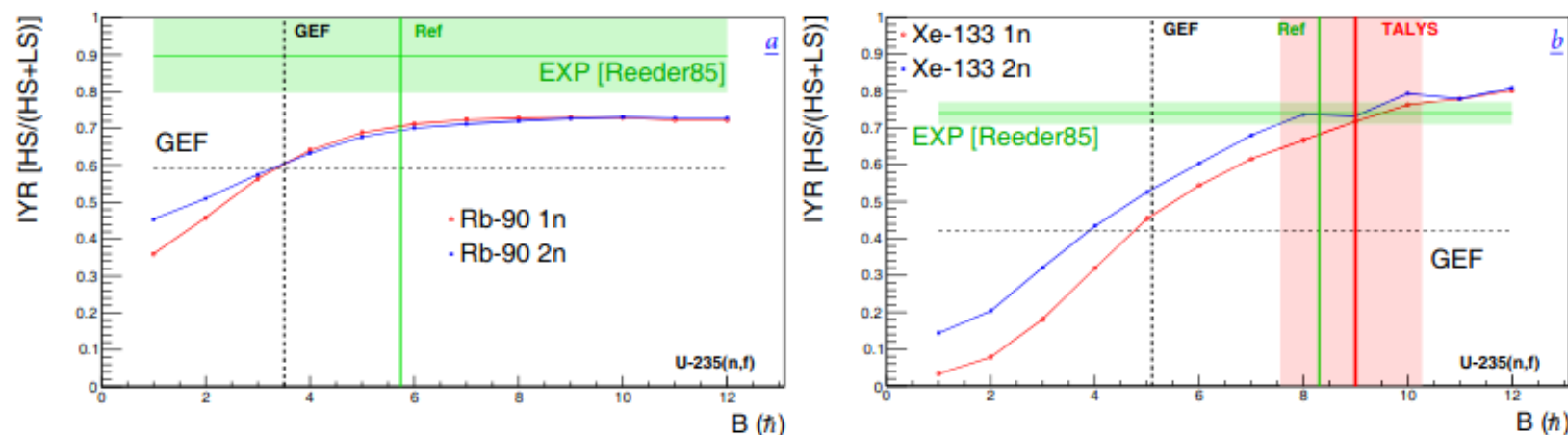


**Fig. 6.** The vertical lines show  $B$ , as extracted from GEF (dashed black line) and the experiment (full green line). (a) The calculations for Rb-90 assuming 1 (red circles) or 2 (blue squares) neutron emissions separately. TALYS fails to meet the high IYR measured reported in ref. [18]. GEF agrees perfectly with the TALYS results if the IYR predicted by GEF is taken as reference. (b) The calculation for Xe-133 where TALYS agrees with the reported  $B$  value of ref. [18]. GEF predicts a lower IYR and is in perfect agreement with TALYS (regarding  $B$ ) if the IYR of GEF is taken as reference.



## More advanced – use GEF to populate J-E<sub>x</sub> matrix

GEF can provide distributions of initial states of fission fragments (see figure).

These can be parameterized to allow for a realistic variation in fragment angular momentum.

The parameters are then varied to find the best value that gives agreement with the experimental observation.

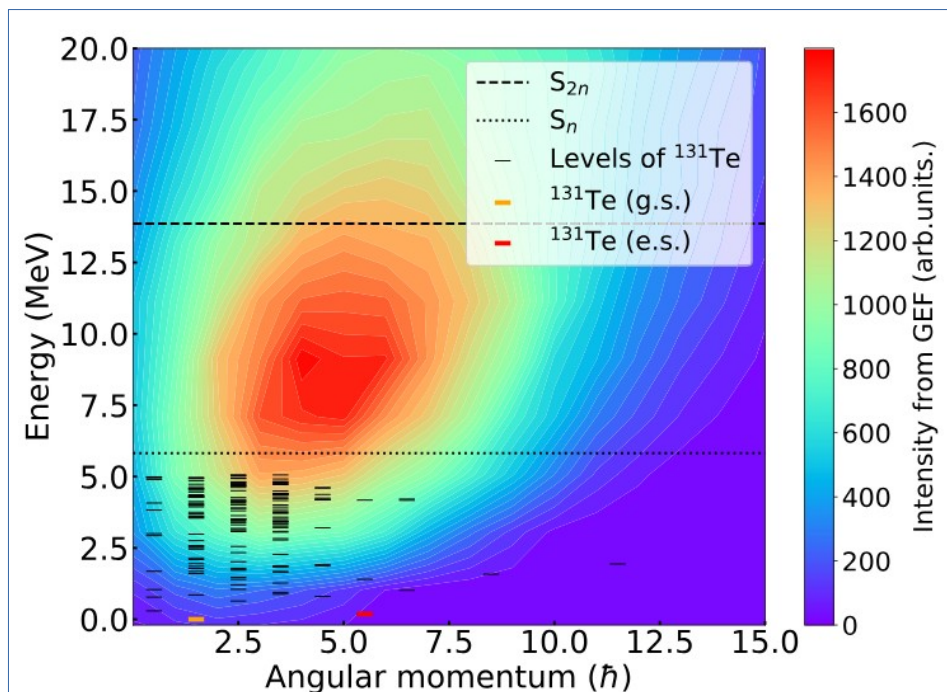
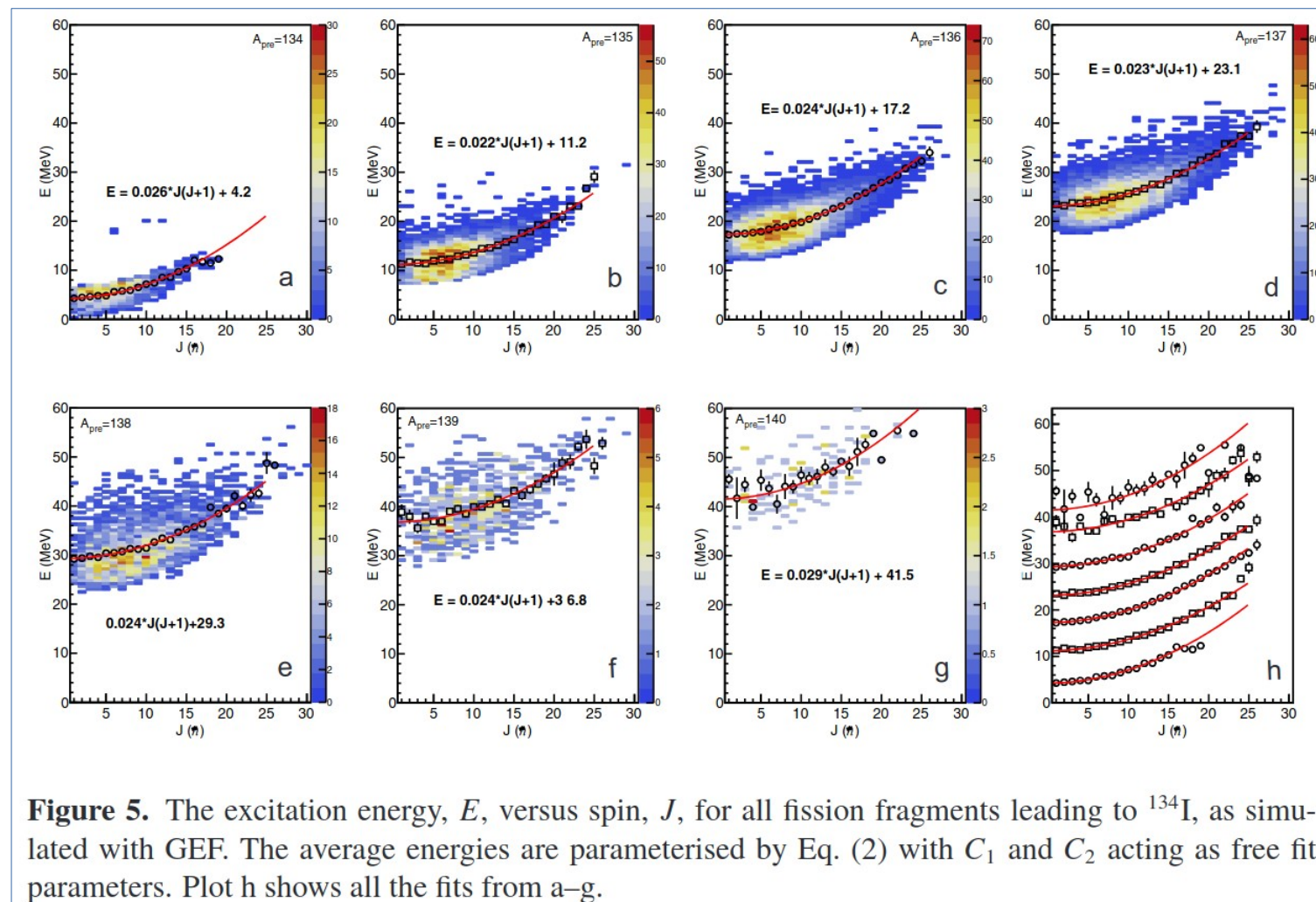


FIG. 1. Excitation energy vs angular momentum population of the primary fission fragment  $^{133}\text{Te}$ , based on GEF calculations for  $^{238}\text{U}(p, f)$  at 25 MeV. The one and two neutron separation energies of  $^{133}\text{Te}$  are represented by a dotted and a dashed line, respectively. The partial level scheme with assigned spins of the de-excitation product  $^{131}\text{Te}$  from the RIPL3 database [14] is added as short black lines. The long-lived excited state (e.s.) and the ground state (g.s.) of  $^{131}\text{Te}$  are marked in red and orange, respectively.

## Surrogate model based on J-E<sub>x</sub> matrixes generated with GEF



Getting the curvature:

$$\bar{E}(J) = C_1 (J^2 + J) + C_2 \propto \frac{\hbar^2}{2\mathcal{I}} J(J+1).$$

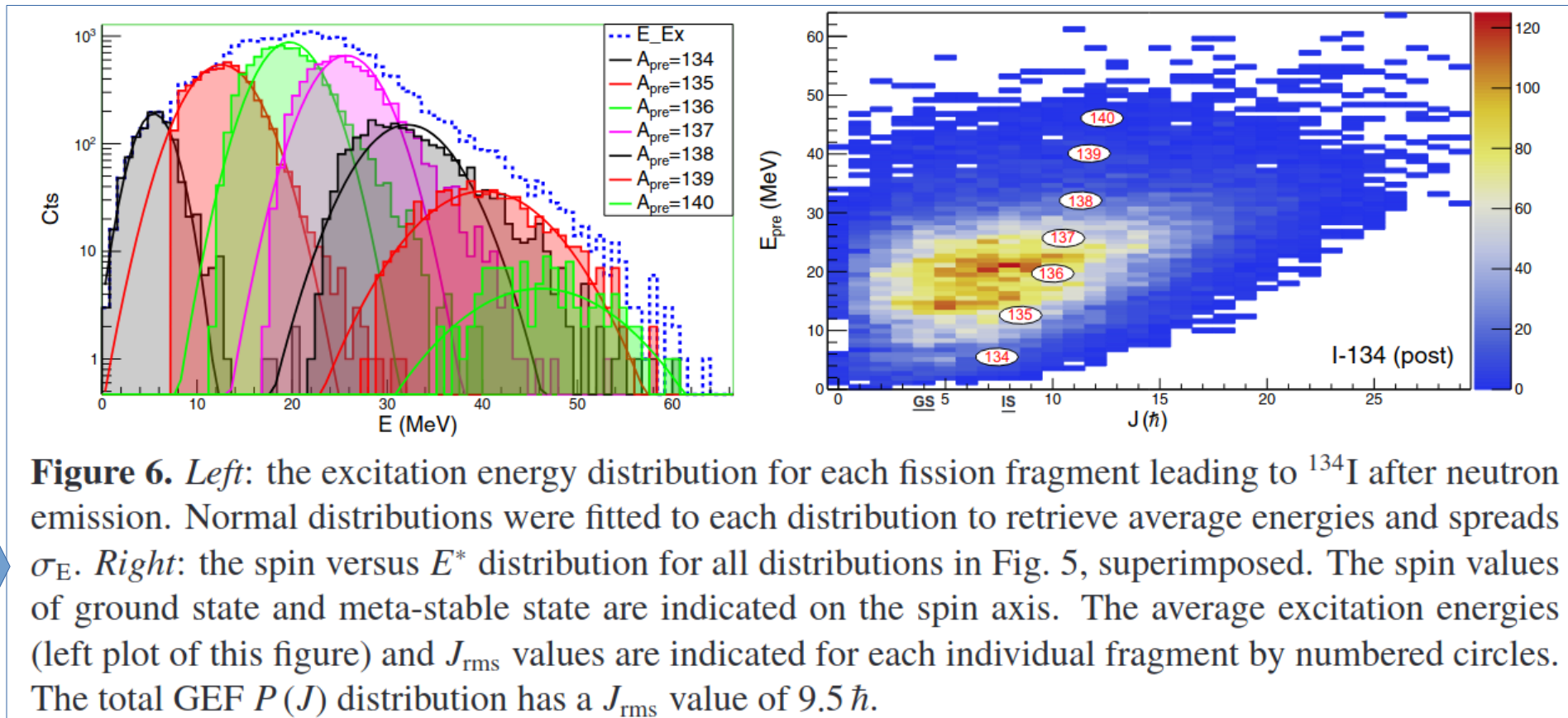
↑  
 $E_{\text{rot}}$



UPPSALA  
UNIVERSITET

## Surrogate model based on $J$ - $E_x$ matrixes generated with GEF

Getting the average energies and spread  $\sigma_E$





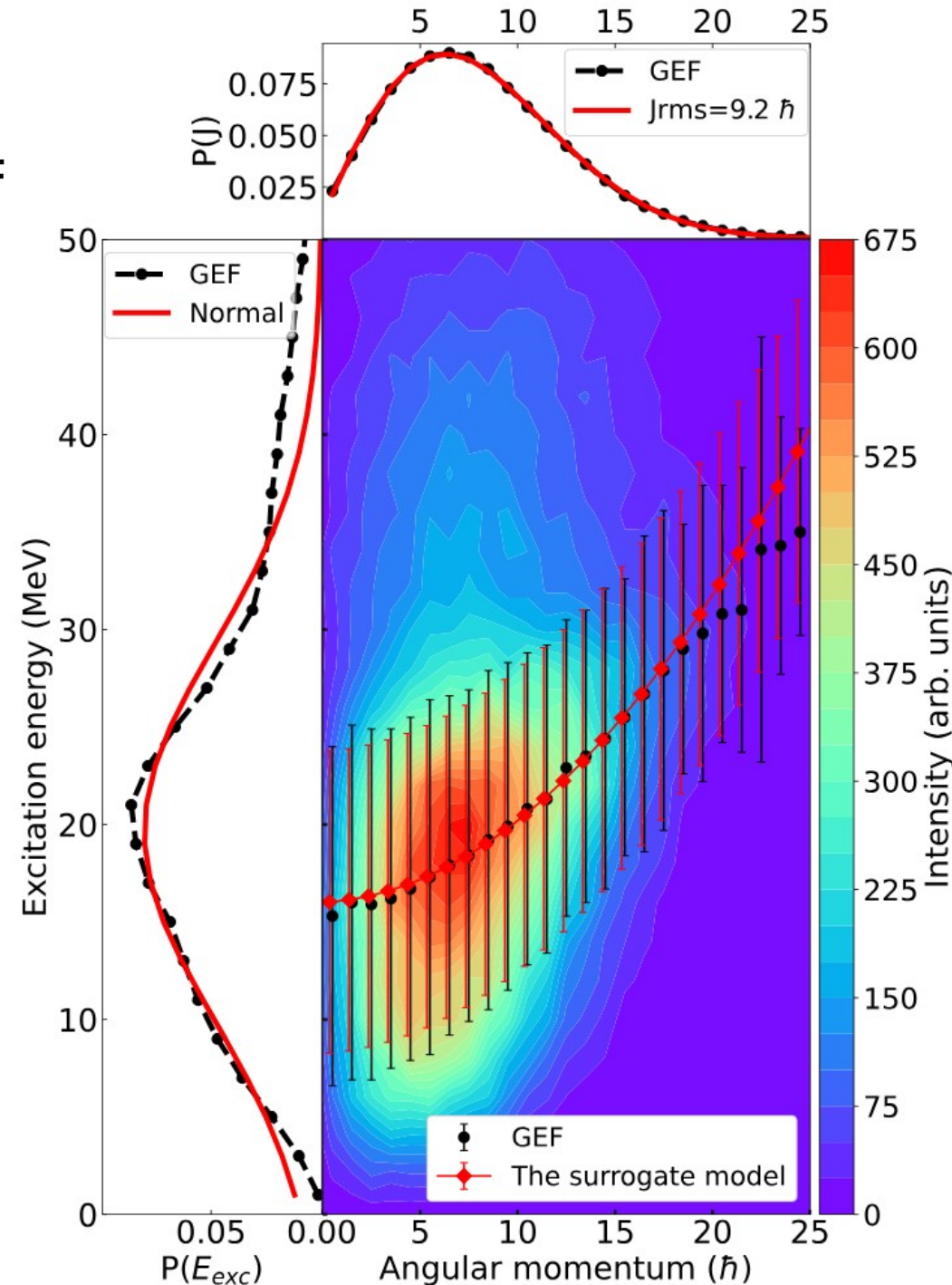
## Surrogate model based on J- $E_x$ matrixes generated with GEF

Finally we add things together:

- excitation energy with offset and rotational energy
- width of excitation energy (Gaussian distribution)

→ 3 parameters

We can populate initial states of fission fragment and vary  $J_{\text{rms}}$  to find best value.





## Using the surrogate model

- Obtain a Ex-J matrix using the surrogate model
- feed the matrix into TALYS and calculate the IYR (using BFM)
- repeat for different  $J_{\text{rms}}$

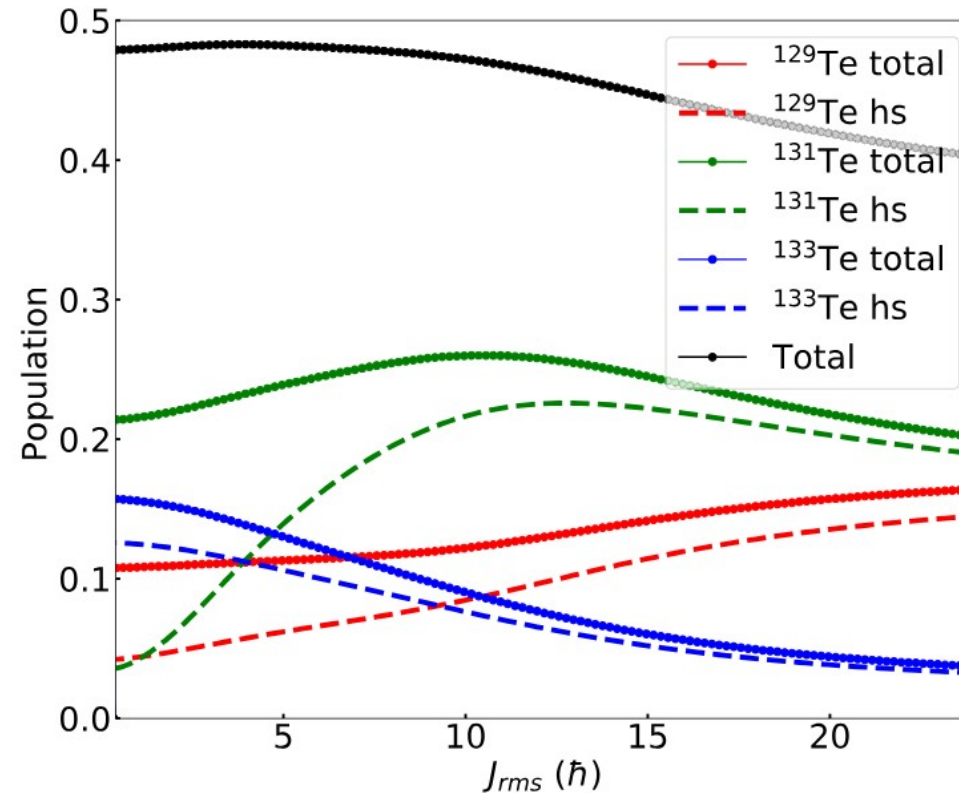


FIG. 4. Populations of the FPs from the deexcitation of FF  $^{133}\text{Te}^*$  as a function of  $J_{\text{rms}}$ .

## Using the surrogate model

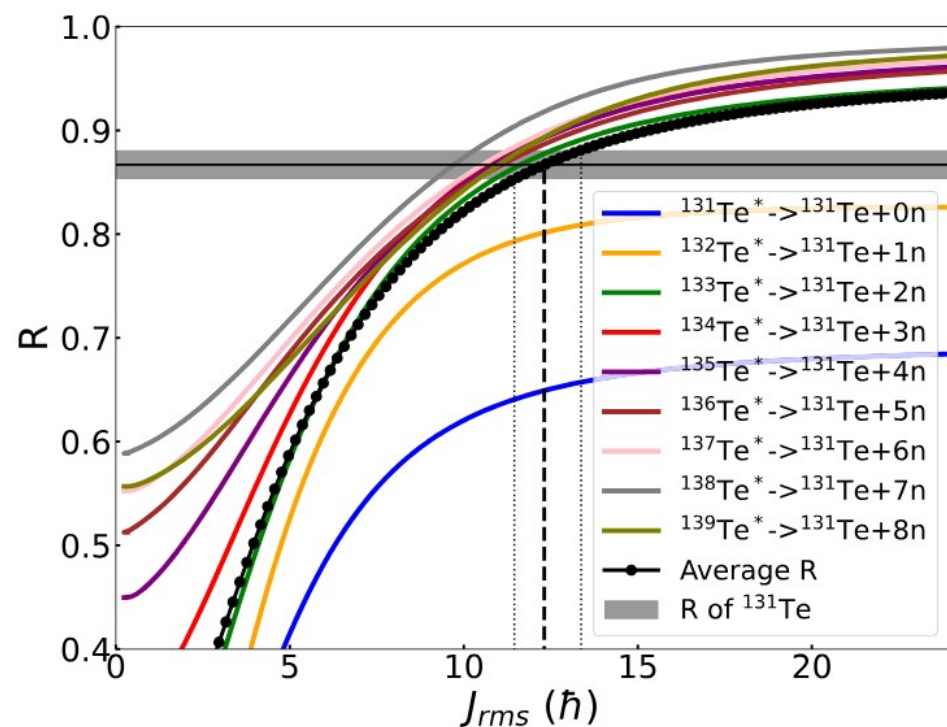


FIG. 5. Calculated IYRs of the FP  $^{131}\text{Te}$  from all excited FFs,  $^{131-139}\text{Te}^*$ , contributing to the production of  $^{131}\text{Te}$ . The horizontal line and gray region represent the measured IYR of the FP  $^{131}\text{Te}$  with uncertainties [26]. The vertical dashed line marks the value of  $J_{\text{rms}}$  where the average curve match the measured ratio.

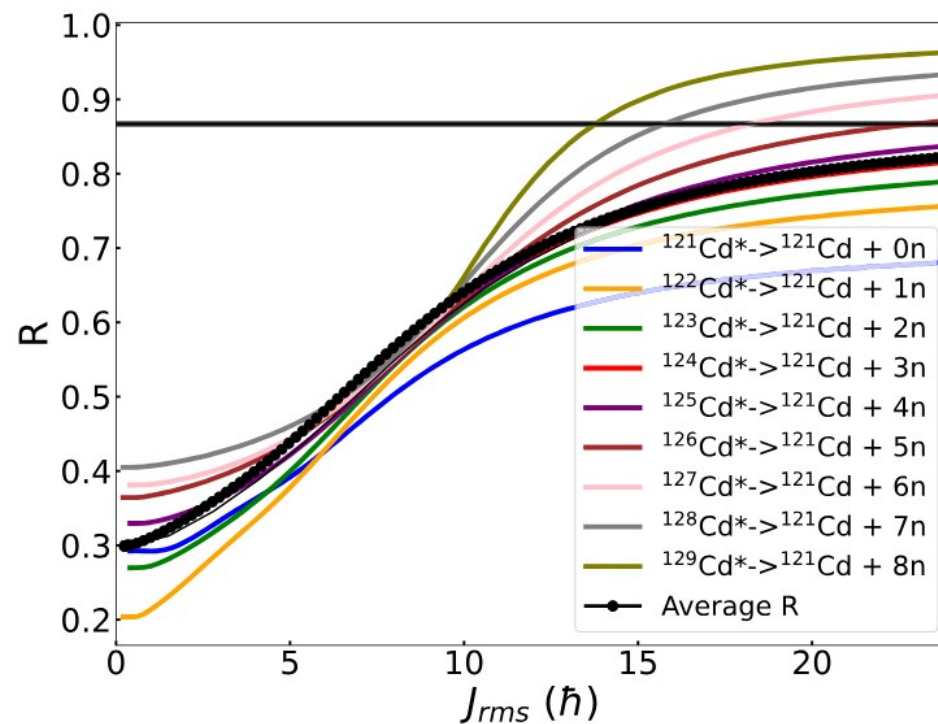
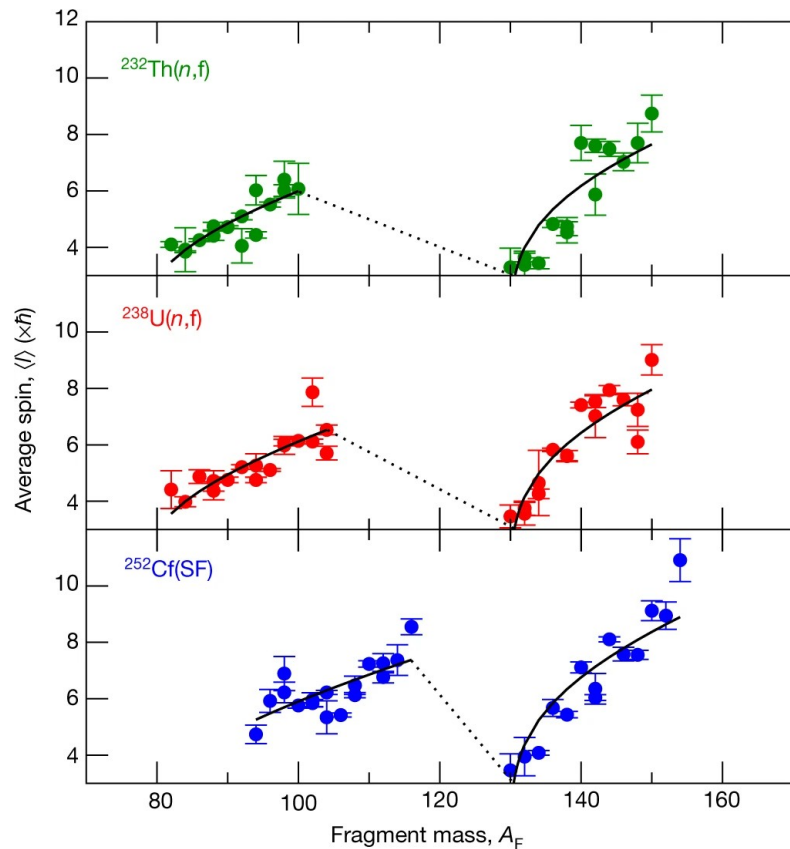
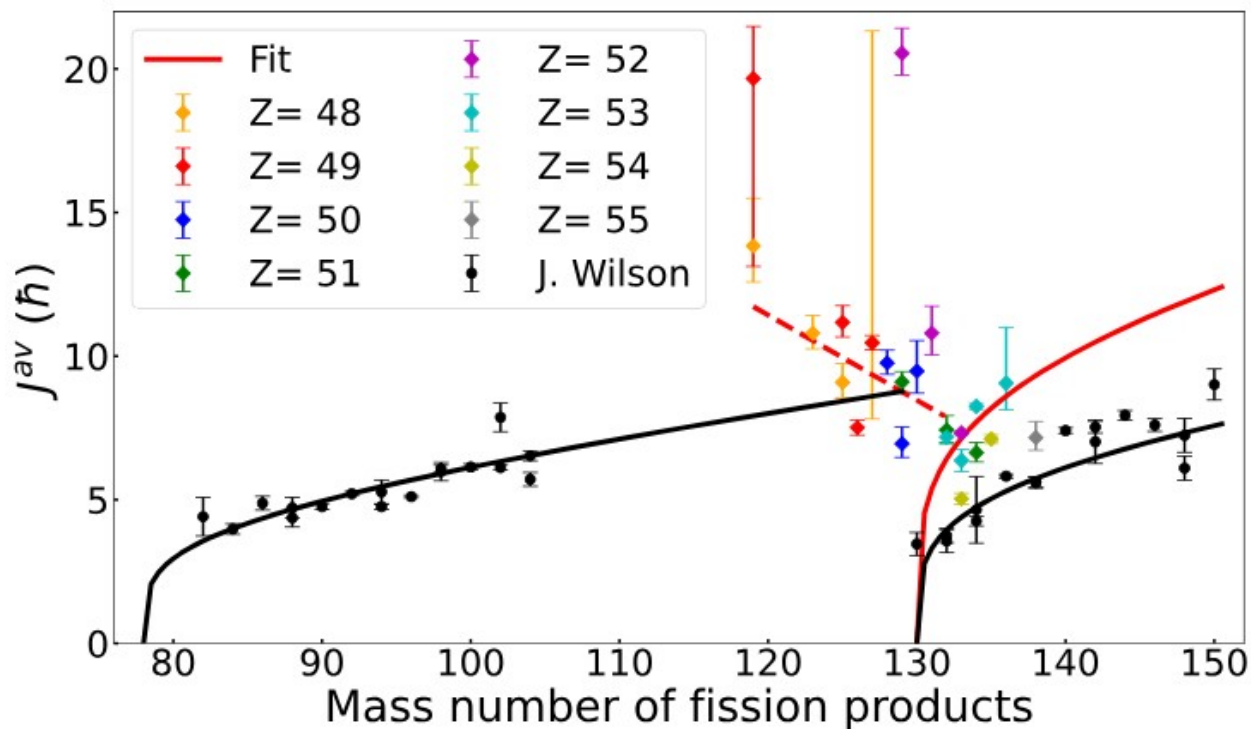


FIG. 6. Calculated IYRs of the FP  $^{121}\text{Cd}$  from all excited FFs,  $^{121-129}\text{Cd}^*$ , contributing to the production of  $^{121}\text{Cd}$ . The horizontal line and gray region represent the measured IYR of the FP  $^{121}\text{Cd}$  with uncertainties [26].

## Results and comparison to Wilson et al.



J. Wilson et al., “Angular momentum generation in nuclear fission”, Nature **590**, 566 (2021)



This result then nicely connects to the question of CN spin impact on FF spin.

It seems the FF spin as function of mass is a sawtooth + a CN spin contribution + possible nuclear shape effects

**Ok, that is a possible approach. But: are the assumptions correct?**

In particular:

How good is TALYS – i.e. the models and assumptions used by the code – in reproducing IYR?

Hard to know in fission (we end up in a circular argument) in what states the fragments are.

➡ Let's look at other cases where TALYS is (likely) good in producing good starting conditions.





# Global comparison between experimentally measured isomeric yield ratios (other than fission) and nuclear model calculations

Goal: investigate the reliability of nuclear models in calculating the IYR of de-exciting nuclei.

Comparison between

- experimentally **obtained IYRs** (from EXFOR), and
- corresponding **TALYS calculations**

Calculations are also repeated changing

TALYS parameters to study their impact on results.

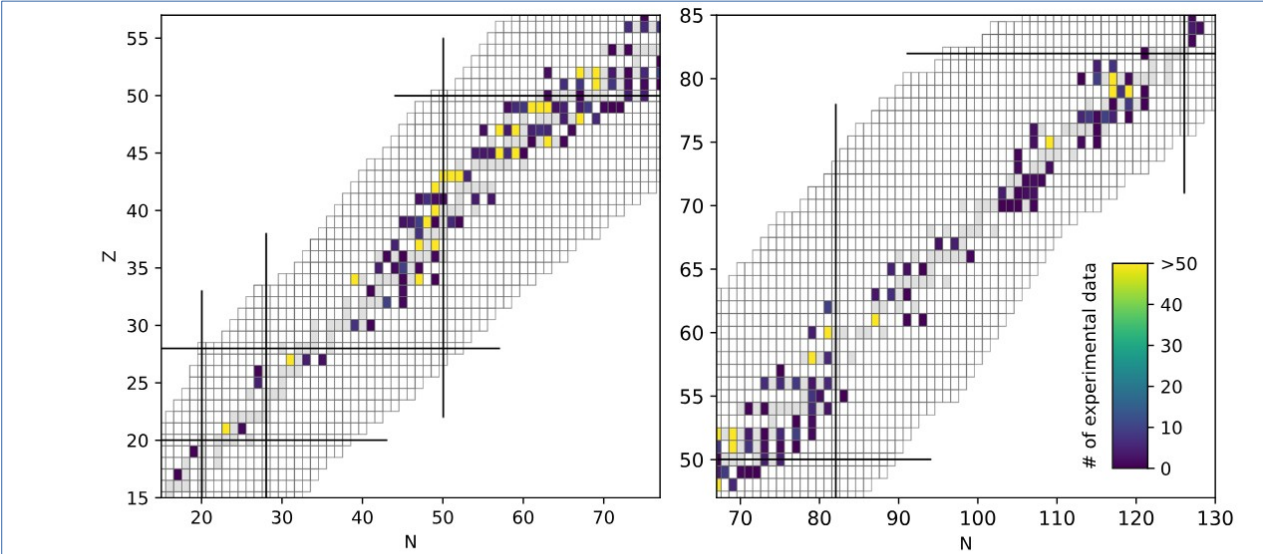


**Fig. 1** Distribution of the nuclei included in the IYR database used in this work on the nuclear chart

**Table 1** Composition of the database divided into the six possible projectile particles, showing both the number of entries and experimental data

Projectile	Entries	Experimental data
n	498	1382
$\gamma$	290	1245
$\alpha$	151	1243
p	138	999
d	40	334
h	13	156
Total	1130	5359



UPPSALA  
UNIVERSITET

Results: on average we find agreement. But ...

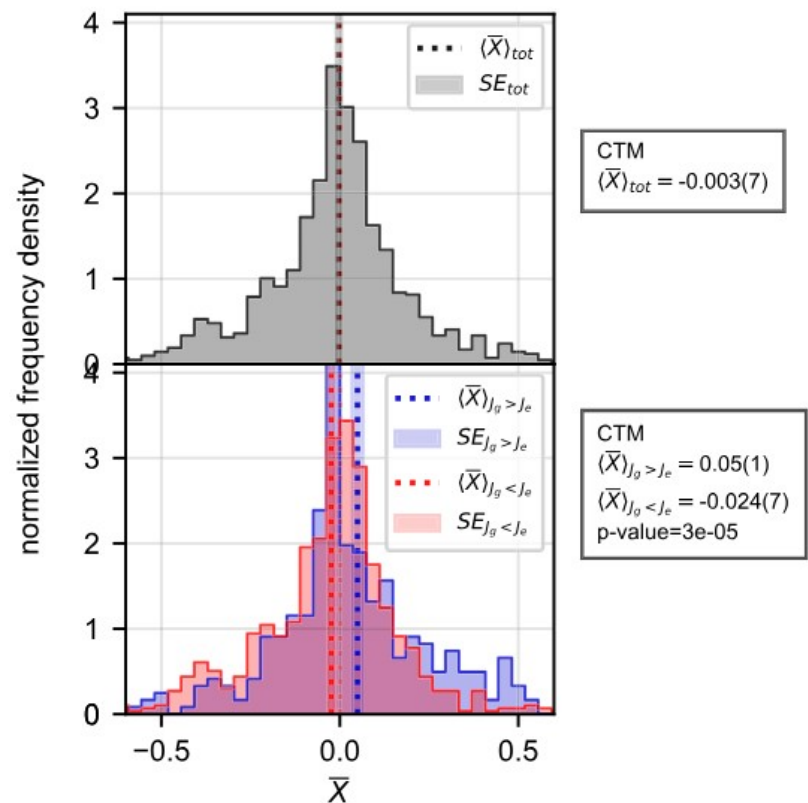


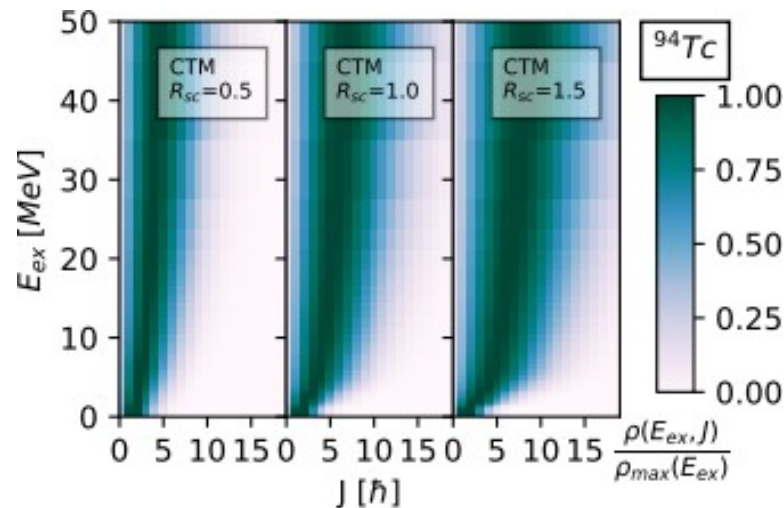
**Table 2** Values of  $\langle \bar{X} \rangle$ ,  $\langle \bar{X} \rangle_{J_g > J_e}$  and  $\langle \bar{X} \rangle_{J_g < J_e}$  for all the six LDM using default settings of TALYS ( $R_{sc} = 1.0$ ). The three microscopic LDM are the Skyrme–Hartree–Fock–Bogoluybov (SHFB), Gogny–Hartree–Fock–Bogoluybov (GHFB), Temperature dependent Gogny–Hartree–Fock–Bogoluybov(TD-GHFB) models [14]

LDM	$\langle \bar{X} \rangle$	$\langle \bar{X} \rangle_{J_g > J_e}$	$\langle \bar{X} \rangle_{J_g < J_e}$
CTM	−0.006 (7)	0.04 (1)	−0.027 (7)
BFM	−0.009 (6)	0.04 (1)	−0.032 (7)
GSM	−0.006 (1)	0.05 (1)	−0.029 (7)
SHFB	−0.016 (7)	0.06 (1)	−0.047 (7)
GHFB	−0.025 (7)	0.06 (1)	−0.055 (7)
TD-GHFB	−0.015 (7)	0.07 (1)	−0.051 (6)

... independent of the used NLD,  
the default calculations **over-predict** the population of the high-spin state.



As an attempt to solve this: squeeze the spin distribution in the NLD towards lower values



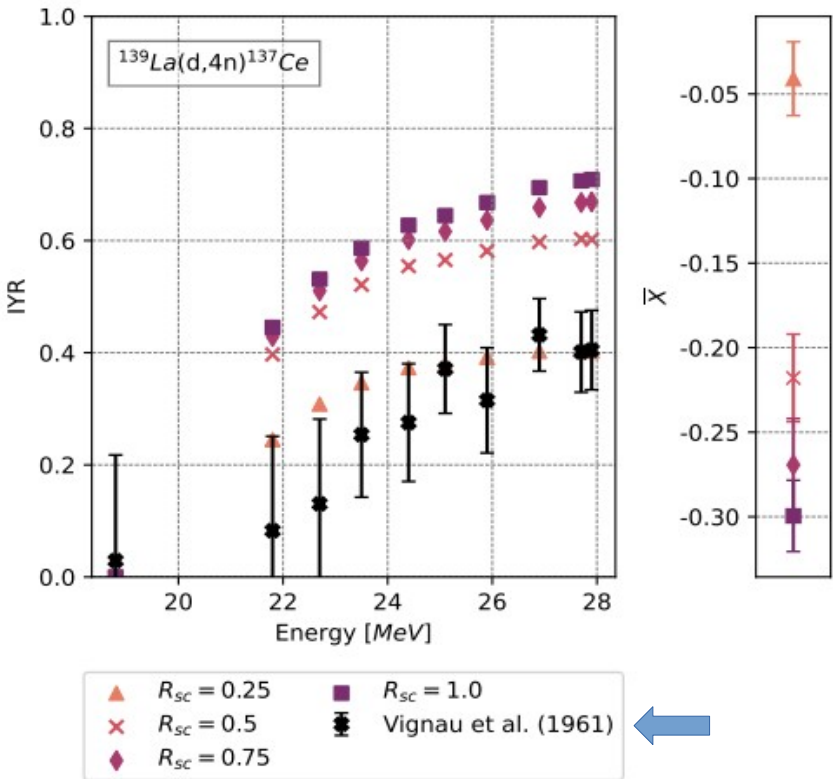
We find that a significant reduction of the spin-width distribution (rspincutoff,  $R_{sc}$ ) is needed to (on average) reproduce the experimental data.

Ground and isomeric state information for  $^{137}_{58}\text{Ce}$

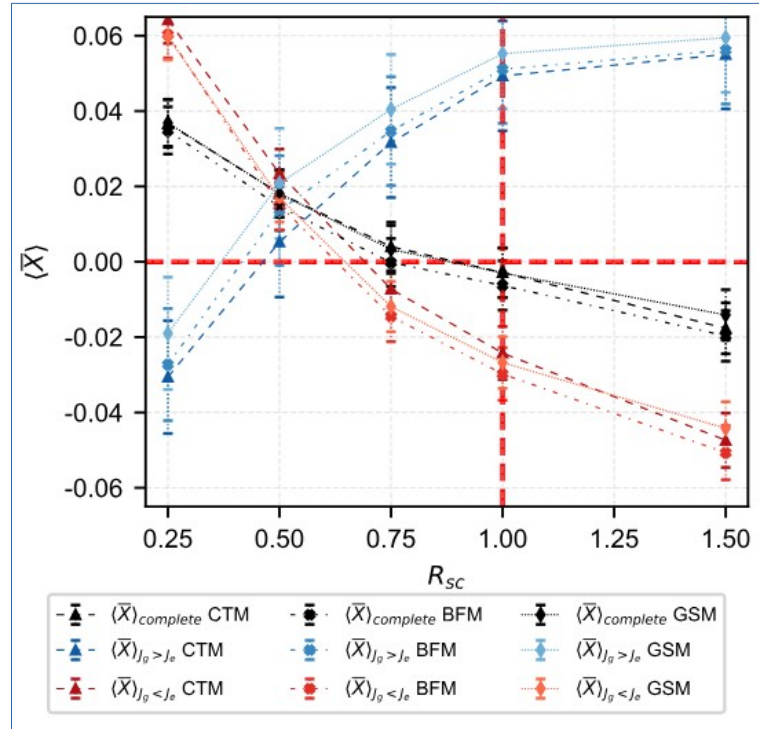
E(level) (MeV)	J $\pi$	Mass Excess (keV)	T <sub>1/2</sub>	Decay Modes
0.0	3/2+	-85918.8 4	9.11 h 3	$\epsilon+\beta+ \approx 100\%$
0.2543	11/2-	-85664.5 4	34.80 h 3	IT = 99.23% $\epsilon+\beta+ \approx 0.77\%$

From NUDAT 3.0

Note: proton-rich case

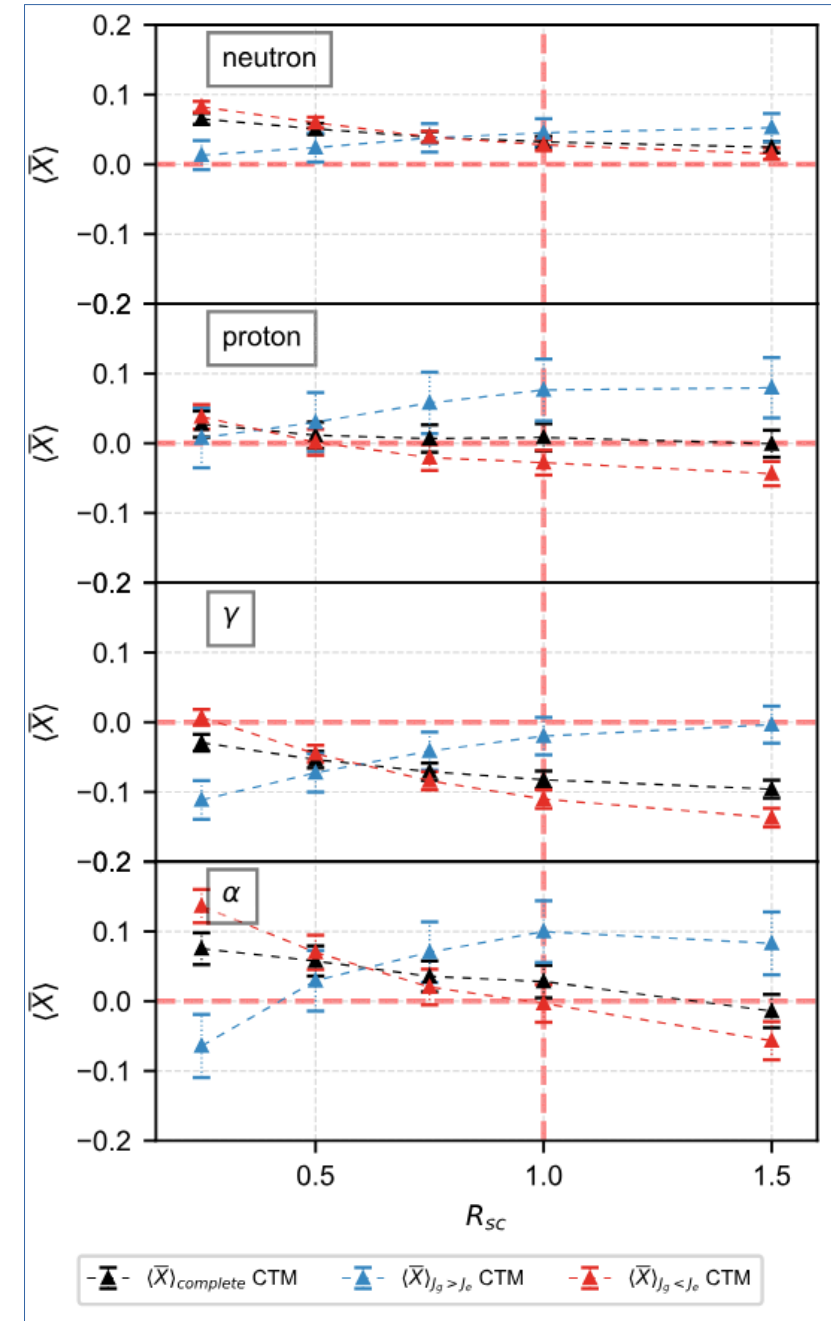


## Result: spin width distribution needs to be reduced



We find a similar trend for all the LDMs, with the convergence of the  $\langle X \rangle$  values for  $R_{sc} \approx 0.5$ .

This holds (more or less) for all studied incident particles.





## What next? Not ordered by calendar time ....

### Experimental:

- Extend IYR database especially in the symmetry and low mass region using  $^{232}\text{Th}(\alpha, f)$ .
- Measure IYR from (n,f) and SF (IGISOL and/or FRS-CSC)

### Computational:

- Perform de-excitation calculation for FF using a model for FF angular momentum ...  
(based on the sawtooth observed by Wilson et al. but extend to account for CN spin)  
... and compare with experimental data.
- Test sensitivity to NLD models and spin width distribution (spin cut-off).



## Acknowledgements

**Thanks!**

Results presented here are based on the PhD theses of **Andreas Mattera** (2017), **Vasileios Rakopoulos** (2018), **Zhihao Gao** (2023), **Simone Cannarozzo** (June 2025)

All work is done in close collaboration with the **IGISOL group** of the University of Jyväskylä.  
We acknowledge the staff of the Accelerator Laboratory of University of Jyväskylä (JYFL-ACCLAB) for providing excellent beams.

### **This work is/was supported by**

- the Swedish Research Council (multiple grants),
- the Research Council of Finland (multiple grants),
- the Swedish Centre for Nuclear Technology (SKC),
- the Swedish Radiation Safety Authority (SSM),
- the Euratom research and training program 2014-2018 under grant agreement No. 847594 (ARIEL).
- the European Union's Horizon 2020 Programme  
(Grant agreement 771036 ERC CoG MAIDEN and 861198-LISA-H2020-MSCA-ITN-2019).



UPPSALA  
UNIVERSITET